

# Does economic optimisation explain LAI and leaf trait distributions across an Amazon soil moisture gradient?

Sophie Flack-Prain<sup>1</sup>  | Patrick Meir<sup>1,2</sup> | Yadvinder Malhi<sup>3</sup> | Thomas L. Smallman<sup>1,4</sup> | Mathew Williams<sup>1,4</sup>

<sup>1</sup>School of GeoSciences, University of Edinburgh, Edinburgh, UK

<sup>2</sup>Research School of Biology, Australian National University, Canberra, ACT, Australia

<sup>3</sup>Environmental Change Institute, School of Geography and the Environment, University of Oxford, Oxford, UK

<sup>4</sup>National Centre for Earth Observation, University of Edinburgh, Edinburgh, UK

## Correspondence

Sophie Flack-Prain, School of GeoSciences, University of Edinburgh, Edinburgh, UK.  
Email: s.flack-prain@ed.ac.uk

## Funding information

Natural Environment Research Council, Grant/Award Number: NE/K002619/1 and NE/J011002/1; Australian Research Council, Grant/Award Number: DP170104091; National Centre for Earth Observation, Grant/Award Number: NE/R016518/1; UKSA project Forests 2020; Royal Society Wolfson; UK Met Office; Newton Fund; CSSP-Brazil project; Gordon and Betty Moore Foundation; ERC Advanced Investigator Award

## Abstract

Leaf area index (LAI) underpins terrestrial ecosystem functioning, yet our ability to predict LAI remains limited. Across Amazon forests, mean LAI, LAI seasonal dynamics and leaf traits vary with soil moisture stress. We hypothesise that LAI variation can be predicted via an optimality-based approach, using net canopy C export (NCE, photosynthesis minus the C cost of leaf growth and maintenance) as a fitness proxy. We applied a process-based terrestrial ecosystem model to seven plots across a moisture stress gradient with detailed in situ measurements, to determine nominal plant C budgets. For each plot, we then compared observations and simulations of the nominal (i.e. observed) C budget to simulations of alternative, experimental budgets. Experimental budgets were generated by forcing the model with synthetic LAI timeseries (across a range of mean LAI and LAI seasonality) and different leaf trait combinations (leaf mass per unit area, lifespan, photosynthetic capacity and respiration rate) operating along the leaf economic spectrum. Observed mean LAI and LAI seasonality across the soil moisture stress gradient maximised NCE, and were therefore consistent with optimality-based predictions. Yet, the predictive power of an optimality-based approach was limited due to the asymptotic response of simulated NCE to mean LAI and LAI seasonality. Leaf traits fundamentally shaped the C budget, determining simulated optimal LAI and total NCE. Long-lived leaves with lower maximum photosynthetic capacity maximised simulated NCE under aseasonal high mean LAI, with the reverse found for short-lived leaves and higher maximum photosynthetic capacity. The simulated leaf trait LAI trade-offs were consistent with observed distributions. We suggest that a range of LAI strategies could be equally economically viable at local level, though we note several ecological limitations to this interpretation (e.g. between-plant competition). In addition, we show how leaf trait trade-offs enable divergence in canopy strategies. Our results also allow an assessment of the usefulness of optimality-based approaches in simulating primary tropical forest functioning, evaluated against in situ data.

## KEYWORDS

canopy dynamics, fitness proxy, leaf traits, moisture stress, optimisation, tropical rainforests

This is an open access article under the terms of the Creative Commons Attribution License, which permits use, distribution and reproduction in any medium, provided the original work is properly cited.

© 2020 The Authors. *Global Change Biology* published by John Wiley & Sons Ltd

## 1 | INTRODUCTION

Leaf area index (LAI, the total one-sided leaf area per unit ground area) determines canopy light interception, evapotranspiration and energy exchange between the land and atmosphere, driving significant spatial and temporal variability in carbon (C) assimilation (Caldararu et al., 2012; Muraoka et al., 2010; Street et al., 2007; Xu & Baldocchi, 2004). Accordingly, LAI is a key property in the investigation of global biogeochemical cycles for both field and model-based studies (Baldocchi et al., 1996; Carswell et al., 2002; Sellers et al., 1997). Principal determinants of global variation in LAI include moisture stress, photoperiod, temperature and nutrients (Fisher et al., 2012; Grier & Running, 1977; Iio et al., 2014; Jolly et al., 2005; Schleppi et al., 2011; Wright et al., 2013).

However, our ability to simulate spatial and temporal variation in LAI remains limited. Resolving this knowledge gap is important in the tropics (De Weirtdt et al., 2012; Kim et al., 2012) as its forests, for instance those in the Amazon, have a large influence on the global C cycle (Liu et al., 2017; Malhi et al., 2008; Pan et al., 2011) and climate system. Broad patterns across the Amazon basin are clear; mean LAI decreases and LAI seasonality increases with increasing soil moisture stress, as forests shift from humid towards seasonally dry (Araujo-Murakami et al., 2014; Malhi et al., 2014). However, the climate sensitivity of phenological change remains unpredictable.

A key challenge in process-based modelling of LAI in tropical forests is to capture the phenological sensitivity to climatic forcings, via leaf senescence and leaf net primary productivity (NPP). Leaf-out timing and leaf turnover are often dependent on environmental factors including plant available water and radiation (Myneni et al., 2007); however, these processes are highly parameterised within models and lack a clear theoretical underpinning (Table S1). Moreover, many models continue to simulate leaf NPP as a fixed fraction of total NPP (Clark et al., 2011; Thornton & Zimmermann, 2007). Such model structures lack the capacity to actively vary LAI in response to soil moisture stress, particularly within the context of climatic change. As a result, current terrestrial biosphere and ecosystem models predict LAI dynamics poorly for Amazon forests across a range of dry season intensities: in a model data comparison study for this region, Restrepo-Coupe et al. (2017) found that of the models tested (IBIS, ED2, JULES and CLM3.5), only ED2 did not grossly overestimate mean LAI. Indeed, none of the models tested were able to capture dry season changes in LAI for equatorial forests. Xu et al. (2016) similarly found that while the ED2 model (with an updated PFT and hydrology scheme) was able to capture spatial patterns in LAI across the Central American region, it simulated mean LAI c.  $1 \text{ m}^2/\text{m}^2$  higher than MODIS estimates, and its simulated LAI seasonality was lower. However, it is important to note that uncertainty in MODIS LAI estimates is high in tropical regions (Liu et al., 2018; Xu et al., 2018).

The simulation of seasonal and annual LAI dynamics could be usefully improved via an optimality-based approach (Anten, 2016; Thomas & Williams, 2014). Such an approach assumes that plants aim to maximise fitness (i.e. optimise), where fitness is defined as

the capacity to grow, reproduce and survive (Geber & Griffen, 2003; Violle et al., 2007). Within an optimisation framework, leaf, root and stem growth, together with plant traits, are adjusted to maximise plant fitness. Net canopy C export (NCE; or variant of) is a commonly used fitness proxy (Franklin et al., 2009; McMurtrie & Dewar, 2011; McMurtrie et al., 2008). Akin to leaf level C optimisation approaches (Ackerly, 1999; Kikuzawa, 1991), NCE balances canopy level C gain via gross primary productivity (GPP) against C loss via growth ( $\text{NPP}_{\text{Leaf}}$ ) and respiration ( $\text{RM}_{\text{Leaf}}$  and  $\text{RG}_{\text{Leaf}}$ ; leaf maintenance and leaf growth respiration, respectively) (Givnish, 2002; Reich et al., 2009).

$$\text{NCE} = \text{GPP} - \text{NPP}_{\text{Leaf}} - \text{RM}_{\text{Leaf}} - \text{RG}_{\text{Leaf}} \quad (1)$$

The maximisation of NCE is dependent on leaf traits, including but not limited to, photosynthetic capacity, leaf mass per unit area (LMA), leaf maintenance respiration rate and leaf lifespan (Field, 1983; McMurtrie & Dewar, 2011). Leaf traits directly influence the rate of C gain via photosynthetic capacity. Leaf traits also directly influence C losses, including C used for leaf growth via LMA and leaf maintenance respiration via metabolic activity (Thomas et al., 2019). In addition, leaf traits indirectly affect C assimilation and leaf maintenance C costs, through the influence of leaf lifespan on total standing leaf biomass.

Leaf traits vary widely across the Amazon basin. Leaf nitrogen (N) content is associated with photosynthetic capacity and maintenance respiration (Evans, 1989; Reich et al., 2008), varying sevenfold across Amazonia (6–41 mg/g) while LMA varies tenfold (30–299 g/m<sup>2</sup>; Fyllas et al., 2009) and individual leaf lifespans can range from less than 2 months to over 4 years (Reich et al., 1991). Combinations of leaf traits have been shown to exist along a leaf-economic spectrum, exhibiting trade-offs among key trait-based axes of functionality (Wright et al., 2004, 2005; Wright & Westoby, 2002). 'Slow' leaf traits (i.e. long leaf lifespan, high LMA, low photosynthetic capacity and low metabolic rate) typically dominate in evergreen terra-firme forests (e.g. Carswell et al., 2000), while fast leaf traits (i.e. short leaf lifespan, low LMA, high photosynthetic capacity and high metabolic rate) are more prevalent in seasonally dry forests (Fyllas et al., 2009; Givnish, 2002; Poorter & Bongers, 2006; Wright et al., 2001). It is therefore critical to account for spatial variation in leaf traits, and their covariance, when investigating the interaction between NCE, LAI and soil moisture stress across Amazon forests.

Optimality-based canopy models have had some success in predicting mean tropical LAI and its seasonality. For example, Caldararu et al. (2016) present a leaf phenology model which optimises net C assimilation (photosynthesis minus leaf maintenance C costs) as a function of temperature, available light, soil water and leaf ageing. The model was able to explain 98% of spatial variation in tropical forest mean LAI, and 63% of variation in LAI amplitude (for the year 2006; where the model was parameterised on a pixel-by-pixel basis using a Markov Chain Monte Carlo fitting algorithm against MODIS LAI training data for the years 2001–2005). However, Caldararu et al. (2016) did not compare fitted model parameters (which included photosynthetic efficiency, leaf maintenance C costs and

leaf ageing rate) to ground-based estimates, nor did fitted parameters adhere to known inherent co-variation as a result of physiological trade-offs (Osnas et al., 2013). Elsewhere, leaf lifespan has been presented as an emergent property of C optimality modelling, evaluated against observation data (Xu et al., 2017). While optimality-based canopy models have been applied globally, model evaluation against tropical forests' field estimates of C fluxes (i.e. GPP, NPP and respiration) has been limited (Caldararu et al., 2014; Vico et al., 2017). Furthermore, current approaches have yet to explore how observed variation in traits (photosynthetic capacity, LMA, leaf maintenance respiration rate and leaf lifespan) affect C cost and gain dynamics. Until now, a lack of fundamental information on C uptake, allocation, metabolism and plant traits has limited the scope for more detailed optimisation theory testing against tropical forest in-situ data.

To this end, we use the process-orientated terrestrial ecosystem Soil-Plant-Atmosphere model (SPA), to investigate LAI optimality through analysis of plant C and water cycles, for forest plots with detailed C budget measurements across an Amazonian moisture stress gradient. Previous work calibrating SPA to plots across the moisture stress gradient, has shown that modelled C dynamics are consistent with field estimates (Flack-Prain et al., 2019), and therefore provide a basis for model experimentation of C dynamics.

Our key science questions are:

1. How does (a) mean LAI and (b) LAI seasonality impact NCE trade-offs between leaf C costs and C assimilation across the moisture stress gradient?
2. Are in situ LAI measurements consistent with optimality-based predictions?
3. How do trait trade-offs across the leaf economic spectrum impact optimal LAI dynamics?

For question 1, we hypothesise that leaf growth and maintenance C costs increase with mean LAI independent of climate (Figure 1). In the absence of drought, GPP increases with mean LAI (prior to shading effects), making high LAI an optimal strategy. Under high moisture stress, GPP is increasingly limited at higher LAI, resulting in a lower optimal leaf area. With respect to LAI seasonality (see Equation 2), we hypothesise that under low seasonal moisture stress leaf C costs increase with LAI seasonality. High LMA and faster leaf turnover result in higher leaf growth costs. In addition, (annual) GPP decreases as LAI seasonality increases. As a result, we predict aseasonal LAI will be optimal for forests with more consistent year-round rainfall. Conversely, where seasonal moisture stress is high, we predict leaf C costs decline as LAI seasonality increases. Maintenance respiration costs decrease alongside seasonal declines in LAI. GPP does not increase as LAI seasonality declines if GPP is limited by seasonal moisture stress. We therefore hypothesise that higher LAI seasonality will be economically optimal in sites with stronger seasonal climates. As such, we predict that in response to question 2, C cycle dynamics under optimal mean LAI and LAI seasonality (i.e. that which maximises NCE) will reflect and explain in-situ data.

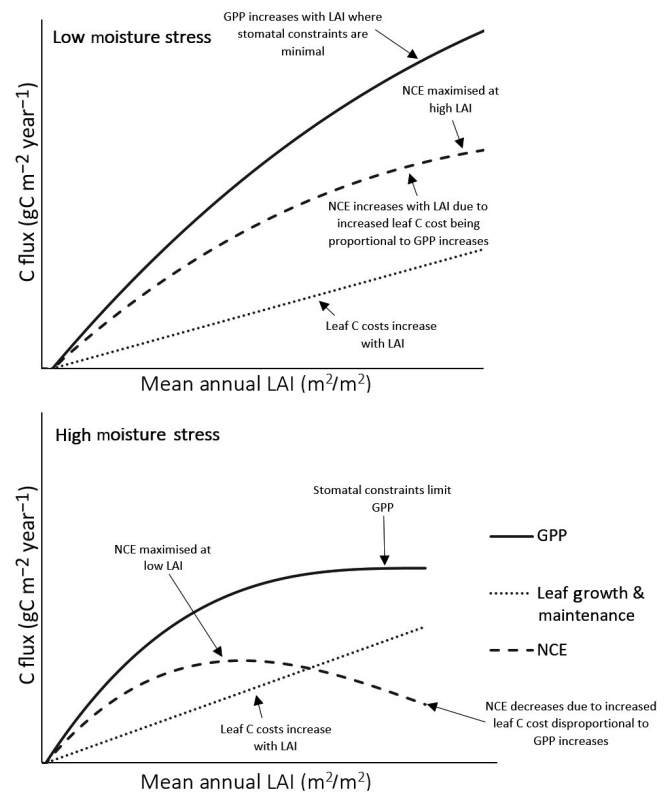


**FIGURE 1** Hypothesised gross primary productivity (GPP), net canopy C export (NCE) and leaf growth and maintenance C costs across a mean leaf area index (LAI) gradient for a typical low and high moisture stress plot. Optimal LAI is lower for high moisture stress plots, due the effect of water limitation on stomatal conductance, consequently limiting GPP and NCE at higher leaf area. GPP and NCE increase with mean LAI for low moisture stress plots as water constraints to stomatal conductance are lower

For question 3, we investigate how NCE responds to changes in leaf traits (photosynthetic capacity, LMA, leaf maintenance respiration rate and leaf lifespan). Leaf traits determine C costs of canopy construction and longevity, which influence the economics of optimisation. Therefore, an alternative hypothesis is that variation in leaf traits will allow aseasonal LAI even in seasonal climates. Optimal leaf traits (i.e. that which maximise NCE) are predicted to match observed trait distributions across the moisture stress gradient. Furthermore, we hypothesise that leaf traits and LAI will be inextricably linked, and that optimal leaf trait strategies will depend on LAI and vice versa.

Optimisation approaches could offer a unique opportunity to reduce uncertainty in predictions of Amazon phenology, and consequently C fluxes. This study will test the suitability of a C economic optimisation approach to predict ecosystem functioning in response to soil water limitation. We use Amazon permanent sample plots with uniquely detailed timeseries measurements of C fluxes and LAI, together with a comprehensive suite of leaf trait estimates (Doughty et al., 2015; Fyllas et al., 2009; Malhi et al., 2015). We simulate a range of mean LAI and LAI seasonalities and evaluate their optimality by comparing their NCE. This approach allows us to present comprehensive

predictions about the sensitivity of NCE to LAI. Furthermore, we are able to present trade-offs in C allocation dynamics, leaf traits and soil moisture stress, referenced against in situ data. We discuss the potential for optimisation approaches to improve earth system model predictions of canopy properties and C cycling.

## 2 | MATERIALS AND METHODS

### 2.1 | Site characteristics

This study uses field data from Amazon forest sites of the Global Ecosystem Monitoring network (GEM; Malhi et al., 2015). We focus on seven 1 ha permanent sample plots along moisture stress gradients in the east and west Amazon, distributed across four locations (Table 1). Moisture stress across plots is quantified using maximum climatological water deficit (MCWD), a measure of seasonal water deficit where more negative values relate to larger water deficit, and potentially greater moisture stress (the focal MCWD gradient spans  $-86$  to  $-498$  mm; see Data S1, for MCWD equation). Soil and species composition differs between localised plots, with little evidence of anthropogenic disturbance (Malhi et al., 2015). A short description of each plot is given here, with further details on site characteristics available in Aragao et al. (2009), Doughty et al. (2015), Quesada et al. (2012), Metcalfe et al. (2010), Araujo-Murakami et al. (2014), Malhi et al. (2014, 2015) and Rocha et al. (2014).

Core terra-firme Amazon forest plots, CAX04 and CAX06 are located in the Caxiuanã National Forest in Para State, Brazil and occupy the least moisture stressed zone of the gradient (MCWD  $-86$  mm). TAM05 and TAM06, located in the Tambopata Biological Reserve in the Madre de Dios region of Peru, are subject to a moderate dry season (MCWD  $-256$  mm). Transitional forest plots—KEN01 and KEN02—are situated in the Hacienda Kenia in Guarayos Province, Santa Cruz, Bolivia, and are subject to a more intense dry season (MCWD  $-342$  mm). The Tanguro plot, located in the Fazenda Tanguro, Mato Grosso State, Brazil, occupies the highest moisture stress zone along the gradient (MCWD  $-498$  mm).

### 2.2 | LAI and leaf trait dynamics across the soil moisture gradient

We used linear regression models to provide an overview of the spatial covariation of observed annual mean LAI, LAI seasonality and leaf traits across the MCWD gradient (see Data S1, for full details on LAI and leaf trait measurements). In the analysis, we also included precipitation seasonality (%) as a characteristic of precipitation regime (see Section 2.5 for calculation).

### 2.3 | The Soil-Plant-Atmosphere model

SPA is a process-based hydrodynamic, terrestrial ecosystem model (Williams et al., 1996), which has previously been calibrated and evaluated against measured C and water fluxes for moist tropical forests in Caxiuanã (eastern Amazon) and Manaus (central Amazon; Fisher et al., 2007; Williams et al., 1998). The pathways through which soil moisture LAI, and leaf traits impact C assimilation and leaf C costs (i.e. NCE) in SPA are summarised in Figure 2, and are described below.

SPA simulates the vertical distribution of canopy layer-specific energy-balance, heat and mass exchange, including photosynthesis and transpiration for up to 10 canopy layers (Bonan et al., 2014; Williams et al., 1996). Each canopy layer in SPA is further partitioned between sunlit and shaded fractions. The radiative transfer scheme determines the canopy interception of radiation (following Beer–Lambert's law) and its subsequent transmittance, reflectance and absorption of long wave, near infra-red and direct and diffuse photosynthetically active radiation for each canopy layer and the soil surface (Williams et al., 1998). The long wave radiation balance is updated by the impact of the soil and canopy energy balance on temperature (Smallman et al., 2013). Boundary layer exchange is subject to the decay of wind speed above and within the canopy profile modified by the impact of the surface energy balance on turbulent exchange (Smallman et al., 2013). The vertical distribution of N within the canopy is represented as an

**TABLE 1** Environmental characteristics summary of GEM network Amazon permanent sample plots (Malhi et al., 2015). Climate measures including maximum climatological water deficit (MCWD) are derived from local weather station data gap filled with ERA interim data for the years 2009–2010 (Dee et al., 2011)

|                               | Caxiuanã Control | Caxiuanã Tower | Tambopata V | Tambopata VI | Kenia Wet | Kenia Dry | Tanguro   |
|-------------------------------|------------------|----------------|-------------|--------------|-----------|-----------|-----------|
| RAINFOR site code             | CAX04            | CAX06          | TAM05       | TAM06        | KEN01     | KEN02     | —         |
| Latitude (°N)                 | −1.716           | −1.737         | −12.831     | −12.839      | −16.016   | −16.016   | −13.077   |
| Longitude (°E)                | −51.457          | −51.462        | −69.271     | −69.296      | −62.73    | −62.73    | 52.386    |
| MCWD (mm)                     | −85.5            | −85.5          | −256.2      | −256.2       | −342.3    | −342.3    | −498.1    |
| Precipitation seasonality (%) | 166.1            | 166.1          | 287.9       | 287.9        | 391.2     | 391.2     | 126.8     |
| Soil type                     | Vetic Acrisol    | Ferralsol      | Cambisol    | Alisol       | Cambisol  | Cambisol  | Ferralsol |
| Sand (%)                      | 83.69            | 32.54          | 40          | 2            | 58.05     | 55.48     | 45.73     |
| Clay (%)                      | 10.68            | 53.76          | 44          | 46           | 19.13     | 18.25     | 48.9      |





coefficients. SPA hydraulic conductance parameters derived from detailed field measurements at an Amazon moist forest site were used in model runs for all plots (Fisher et al., 2006, 2007; Rowland, Harper, et al., 2015). Hydraulic conductance parameters include stem conductance, minimum leaf water potential, intrinsic water use efficiency, leaf capacitance and root resistivity. Hourly meteorological forcing data were supplied from weather stations located within 1 km of the study plots. Data gaps in air temperature, wind speed, shortwave radiation and vapour pressure deficit records which were less than six consecutive hours were estimated by spline interpolation. Data gaps greater than 6 hr, or gaps in precipitation measurements were filled using hourly spline-interpolated and bias corrected ERA-Interim data (Dee et al., 2011). Solar zenith angle was accounted for when interpolating solar radiation values. Monthly LAI measurements were scaled to daily estimates via linear interpolation to force simulated LAI.

Timeseries field measurements of soil moisture and leaf litterfall were used to calibrate simulated soil water drainage parameters and leaf fall parameters respectively. Within SPA, the empirical model used to simulate soil hydraulics (Saxton et al., 1986, equation 10) was calibrated by adjusting the slope of the interaction between soil texture and water retention, to reflect tropical soil moisture dynamics (to within standard error estimates of annual mean soil moisture). Modelled leaf litterfall was calibrated to accurately simulate litterfall period and amplitude (within standard error estimates of annual litterfall), using field measurements to retrieve model parameters on leaf fall timing, duration and potential leaf lifespan (Table 2).

SPA was evaluated against independent field estimates of annual ecosystem C fluxes, including NPP, GPP, NCE and autotrophic respiration. Total NPP and autotrophic respiration were calculated as the sum of measured leaf, root and wood NPP and respiration respectively. GPP was calculated as the sum of total measured NPP and autotrophic respiration, and NCE was calculated as the sum of measured root and wood NPP and respiration (i.e. GPP minus leaf NPP and respiration).

The calculation of model uncertainty as a result of parameter error was limited to that associated with LAI estimates, as the availability of uncertainty estimates for leaf traits and rooting properties was plot-dependent, and there were no uncertainty estimates for hourly meteorological data or soil properties. Model uncertainty estimates were calculated by simulating C fluxes for each plot under the upper and lower standard error of monthly LAI field measurements. Following model calibration, simulated C fluxes were evaluated against field estimates of GPP, respiration and NPP, using linear regression models. Field estimates were derived from a suite of biometric timeseries measurements including dendrometers, root ingrowth cores, infra-red gas analysers and litterfall traps (Doughty et al., 2015), further details of which can be found in Data S1.

## 2.5 | Modelling C cycle sensitivity to LAI and soil moisture stress interactions

We tested whether the maximisation of NCE explained observed mean LAI and LAI seasonality across the MCWD gradient. We forced the model at each plot using a suite of synthetic LAI timeseries, and retrieved the resultant C budget. For each plot, during model experiments, meteorology, soil texture, the fraction of NPP allocated to wood and roots (following leaf NPP allocation), initial C stocks and leaf traits were kept constant. To generate the synthetic LAI timeseries, we systematically varied mean LAI (Figure S2) and LAI seasonality (Figure S3) against the observation data at each plot. First, to vary mean LAI, for each plot, we adjusted the annual mean to between 1 and 8 m<sup>2</sup>/m<sup>2</sup> at 0.5 m<sup>2</sup>/m<sup>2</sup> intervals, conserving the nominal seasonal cycle ( $n = 105$ ; 7 plots  $\times$  15 synthetic LAI timeseries). Second, we constructed synthetic LAI timeseries for each plot ( $n = 63$ ; 7 plots  $\times$  9 synthetic LAI timeseries), which conserved nominal mean LAI, but varied LAI seasonality (Table S2).

The timing of LAI<sub>min</sub> in the synthetic LAI timeseries were aligned with seasonal lows in the observation dataset. LAI seasonality (LAI<sub>s</sub>;

**TABLE 2** Mean leaf area index (LAI), LAI seasonality and leaf traits (leaf N content, photosynthetic capacity  $\kappa_c$ ,  $\kappa_j$  and leaf mass per unit area [LMA]) used to parameterise Soil-Plant-Atmosphere model (SPA), and SPA-calibrated leaf litterfall parameters (leaf fall day, leaf lifespan and leaf fall period) for Amazon permanent sample plots. Leaf fall day is the day of year leaf fall is initiated, leaf lifespan reflects potential lifespan of leaves and leaf fall period is the number of days over which leaf fall occurs. Leaf litterfall parameters were calibrated against GEM field estimates

|         | Field-measured parameters                         |                     |                       |   |   |                         | Calibrated parameters       |                       |                         |
|---------|---|---------------------|-----------------------|---|---|-------------------------|-----------------------------|-----------------------|-------------------------|
|         | Annual mean LAI (m <sup>2</sup> /m <sup>2</sup> ) | LAI seasonality (%) | Leaf N content (mg/g) | $\kappa_c$ ( $\mu\text{mol C g N}^{-1} \text{s}^{-1}$ ) | $\kappa_j$ ( $\mu\text{mol C g N}^{-1} \text{s}^{-1}$ ) | LMA (g/m <sup>2</sup> ) | Leaf fall day (day of year) | Leaf lifespan (years) | Leaf fall period (days) |
| CAX04   | 5.0   | 0.2                 | 19.6                  | 15.4  | 27.7  | 93.0                    | 210                         | 3                     | 150                     |
| CAX06   | 5.2   | 2.2                 | 24.3                  | 13.2  | 23.8  | 87.4                    | 190                         | 1.45                  | 100                     |
| TAM05   | 4.9   | 4.9                 | 24.0                  | 28.9  | 49.9  | 101.0                   | 220                         | 1.3                   | 130                     |
| TAM06   | 4.6   | 8.9                 | 24.8                  | 29.0  | 50.3  | 96.0                    | 230                         | 1.42                  | 100                     |
| KEN01   | 2.8   | 14.1                | 40.4                  | 29.3  | 51.6  | 52.5                    | 200                         | 1.05                  | 100                     |
| KEN02   | 2.2   | 18.4                | 55.3                  | 28.9  | 50.3  | 41.8                    | 180                         | 1.01                  | 100                     |
| Tanguro | 4.1   | 1.6                 | 31.2                  | 30.0  | 53.1  | 64.4                    | 180                         | 1.04                  | 120                     |

%), was calculated as the average difference between monthly LAI and the annual mean:

$$LAI_s = \frac{\sum_{i=1}^n \frac{|LAI_i - \overline{LAI}|}{\overline{LAI}}}{n} \cdot 100, \quad (2)$$

where  $LAI_i$  is LAI for a given month,  $\overline{LAI}$  is nominal mean LAI, and  $n$  is the number of months in the timeseries. Estimates of local precipitation seasonality (used in regression analyses to relate LAI and leaf trait distributions to precipitation regime) were calculated using an analogous equation, where  $LAI_i$  was substituted for precipitation in a given month, and  $\overline{LAI}$  was substituted for mean monthly precipitation.

For each LAI timeseries (observed or synthetic), model simulations were run using local climate data, allowing sufficient iterations for C cycle feedbacks on component C pools to reach steady state (300 years). We computed the interaction between C assimilation, the C cost of leaf growth and maintenance (i.e. GPP and NCE), and mean LAI/LAI seasonality for each plot. We compared nominal annual mean LAI to that under the simulated maximum NCE. We then compared field-estimated and model-simulated NCE under nominal LAI, to the maximum simulated NCE retrieved from synthetic LAI timeseries runs (for mean LAI and LAI seasonality). Field-estimated error was the propagated standard error of components (i.e. GPP, leaf NPP and leaf respiration). Optimal mean LAI and LAI seasonality was defined as that which maximised NCE under the plot conditions.

## 2.6 | Leaf trait interactions with NCE along soil moisture gradients

We tested the impact of leaf traits on optimal LAI across the MCWD gradient. We focused on exploring the extremes of the moisture gradient, choosing plots with typically drier (KEN02) and moister (CAX04) climate and soils to simplify the analysis. We used the fast leaf traits observed at the drier KEN02 plot (i.e. short leaf lifespan, low LMA, high photosynthetic capacity and high metabolic rate), and the slow leaf traits nominal at the moister CAX04 plot (i.e. long leaf lifespan, high LMA, low photosynthetic capacity and low metabolic rate; Table 2), to construct model forcings for a fast and slow leaf trait cohort. At both plots, we forced the model with the fast and slow leaf trait cohort, under the suite of synthetic LAI timeseries outlined in the previous section ( $n = 100$ ; for mean LAI 2 plots  $\times$  15 synthetic LAI timeseries  $\times$  2 leaf trait strategies, plus for LAI seasonality, 2 plots  $\times$  10 synthetic LAI timeseries  $\times$  2 leaf trait strategies) and retrieved simulated NCE. As before, for each plot, we kept meteorology, soil texture, the fraction of NPP allocated to wood and roots, and initial C stocks constant. We compared the interaction between NCE and mean LAI/LAI seasonality, under the different leaf trait cohorts, on drier and moister soils. We then contrasted field-estimated and model-simulated NCE under nominal LAI leaf trait distributions, to the

maximum simulated NCE retrieved from synthetic LAI leaf trait runs.

## 3 | RESULTS

### 3.1 | Model calibration and evaluation

SPA was calibrated to effectively simulate soil moisture and leaf litterfall variation and dynamics across sites (Table 3; Figure 3; Figure S5). SPA-simulated GPP was within field estimate error bounds for five of the seven plots (Figure S5; the disparity between error bounds for the remaining two plots was marginal at 115 and 50 gC m<sup>-2</sup> year<sup>-1</sup> for KEN01 and TAM06, respectively). The GPP-MCWD interaction was consistent between simulated GPP and estimates derived from field measurements (slope of GPP ~ MCWD interaction; SPA =  $2.4 \pm 0.8$ ; GEM =  $2.0 \pm 0.9$ ). Modelled and observed NCE were significantly correlated across plots ( $R^2 = .62$ ,  $p = .04$ ). A breakdown of model performance with respect to leaf, root and wood NPP and respiration, is described in Flack-Prain et al. (2019). Model calibration and evaluation results are presented in full in Data S1.

### 3.2 | LAI and leaf traits trends along the MCWD gradient

Canopy and leaf level properties co-varied across the MCWD gradient (Figure S6; Table 4). Mean annual LAI decreased as

**TABLE 3** Model calibration and evaluation performance for permanent sample plots across an Amazon mean maximum climatological water deficit gradient. Soil-Plant-Atmosphere model forced with observed leaf area index, calibrated using field estimates of leaf litterfall and soil moisture, and evaluated against annual net primary productivity (NPP), gross primary productivity (GPP) and autotrophic respiration. We compare modelled values to field estimates of C fluxes to derive the coefficient of determination,  $p$ -value and the normalised root mean square error

|                           | $R^2$ | $p$   | RMSE (%) |
|---------------------------|-------|-------|----------|
| Evaluation                |       |       |          |
| GPP                       | .36   | .15   | 11.2     |
| $R_a$                     | .59   | .04   | 12.2     |
| NPP                       | .38   | .14   | 12.0     |
| NCE                       | .62   | .04   | 12.8     |
| Calibration               |       |       |          |
| Leaf litterfall           | .99   | <.001 | 2.8      |
| Litterfall range          | .54   | .009  | 23.8     |
| Litterfall peak timing    | .96   | <.001 | 7.1      |
| Soil moisture range       | .35   | .21   | 14.7     |
| Soil moisture peak timing | .98   | <.001 | 10.6     |

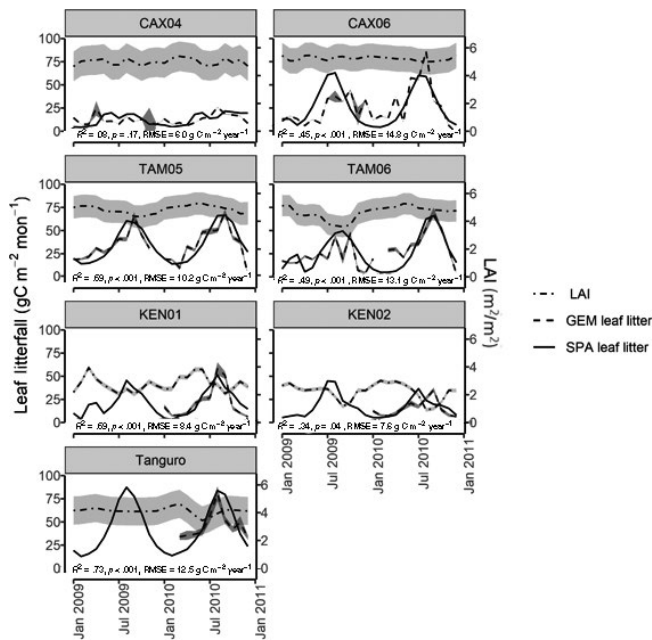


**FIGURE 3** Field-estimated monthly leaf area index, leaf litterfall (GEM) and standard error, compared with Soil-Plant-Atmosphere model (SPA) simulated leaf litterfall for seven plots at four locations across the Amazon basin. SPA leaf litterfall was calibrated against GEM estimates to derive three fixed model drivers relating to the leaf cycle (peak leaf fall timing, leaf fall period and leaf lifespan). GEM leaf litterfall data were available for 2009–2010 for CAX04, CAX06, TAM05, TAM06 and for 2010 only for KEN01, KEN02 and Tanguro.  $R^2$ ,  $p$ -value and RMSE estimates presented are derived from linear regressions between monthly GEM measurements and SPA simulations

precipitation seasonality increased ( $R^2 = .57$ ,  $p = .05$ ). LAI seasonality increased in line with precipitation seasonality ( $R^2 = .87$ ,  $p = .002$ ). Congruously, a significant negative interaction existed between mean annual LAI and LAI seasonality ( $R^2 = .79$ ,  $p = .008$ ). Across the canopy-to-leaf scale, mean annual LAI increased significantly with LMA ( $R^2 = .86$ ,  $p = .002$ ). Mass based foliar N content decreased significantly with mean annual LAI, and increased significantly with LAI seasonality ( $R^2 = .92$ ,  $p < .001$  and  $R^2 = .77$ ,  $p = .009$  respectively). At the leaf-level, a significant negative correlation existed between LMA and mass based foliar N content ( $R^2 = .85$ ,  $p = .003$ ). Correspondingly, mass based foliar N exhibited a significant negative correlation with calibrated leaf lifespan ( $R^2 = .57$ ,  $p = .05$ ).

### 3.3 | Impact of mean LAI on NCE trade-offs across the soil moisture gradient

As a result of leaf C cost and C assimilation trade-offs, high mean LAI was economically deleterious within the model experiment for forest plots occupying drier soils, but remunerative for those occupying moister soils (Figure 4). Simulated leaf C costs (via growth and maintenance) increased linearly with mean LAI. In contrast,

**TABLE 4** Linear regression analyses on the interaction between maximum climatological water deficit (MCWD), precipitation seasonality and in-situ measurements of mean leaf area index (LAI), LAI seasonality, leaf N content, leaf mass per unit area (LMA) and calibrated leaf lifespan across Amazon permanent sample plots

| Interaction   | Slope | $R^2$ | $p$ -value |
|---|-------|-------|------------|
| Mean Annual LAI ~ MCWD                                | +     | .35   | .16        |
| Mean Annual LAI ~ Precipitation Seasonality           | –     | .57   | .05        |
| LAI Seasonality ~ MCWD                                | –     | .13   | .42        |
| LAI Seasonality ~ Precipitation Seasonality           | +     | .87   | .002       |
| Mean Annual LAI ~ LAI Seasonality                     | –     | .79   | .008       |
| LMA ~ MCWD  | +     | .37   | .15        |
| LMA ~ Precipitation Seasonality                       | –     | .23   | .27        |
| LMA ~ Mean Annual LAI                                 | +     | .86   | .002       |
| LMA ~ LAI Seasonality                                 | –     | .49   | .08        |
| LMA ~ Foliar N Content                                | –     | .85   | .003       |
| LMA ~ Calibrated Leaf Lifespan (log-log)              | +     | .39   | .14        |
| Foliar N Content ~ MCWD                               | –     | .29   | .21        |
| Foliar N Content ~ Precipitation Seasonality          | +     | .49   | .08        |
| Foliar N Content ~ Mean Annual LAI                    | –     | .92   | <.001      |
| Foliar N Content ~ LAI Seasonality                    | +     | .77   | .009       |
| Foliar N Content ~ Calibrated Leaf Lifespan (log-log) | –     | .57   | .05        |
| Calibrated Leaf Lifespan ~ MCWD                       | +     | .49   | .08        |
| Calibrated Leaf Lifespan ~ Precipitation Seasonality  | –     | .20   | .31        |
| Calibrated Leaf Lifespan ~ Mean Annual LAI            | +     | .28   | .23        |
| Calibrated Leaf Lifespan ~ LAI Seasonality            | –     | .30   | .20        |

simulated GPP increased with mean LAI for five of the seven plots. The rate of GPP increase slowed as mean LAI increased (Figure 4). At Tanguro and KEN02 (which occupy drier soils), GPP did not increase with mean LAI beyond an upper limit ( $5.5\text{--}6.0\text{ m}^2/\text{m}^2$ ); at higher LAI, GPP declined towards zero. The modelled decline of GPP to zero was due to reduced C availability for non-foliar growth (at high mean LAI) leading to an eventual collapse in fine root biomass stocks, whereby canopy function was no longer supported. The simulated response of leaf C costs and C assimilation to mean LAI caused NCE to be progressively reduced at high mean LAI as soil moisture stress strengthened. Consequently, simulated optimal mean LAI (i.e. LAI at which NCE was maximised;  $\text{LAI}_{\text{Opt}}$ ) declined as moisture stress increased (Figure 5a; mean  $\text{LAI}_{\text{Opt}} \sim \text{MCWD}$   $R^2 = .72$ ,  $p = .02$ ).



**FIGURE 4** Model-simulated net canopy C export (NCE), gross primary productivity (GPP) and leaf growth and maintenance C costs, for each plot along an Amazon maximum climatological water deficit gradient, forced with synthetic leaf area index (LAI) timeseries ranging in mean LAI. Data points are field estimates of NCE, GPP and leaf growth and maintenance. Error bars show the propagated error of summed components

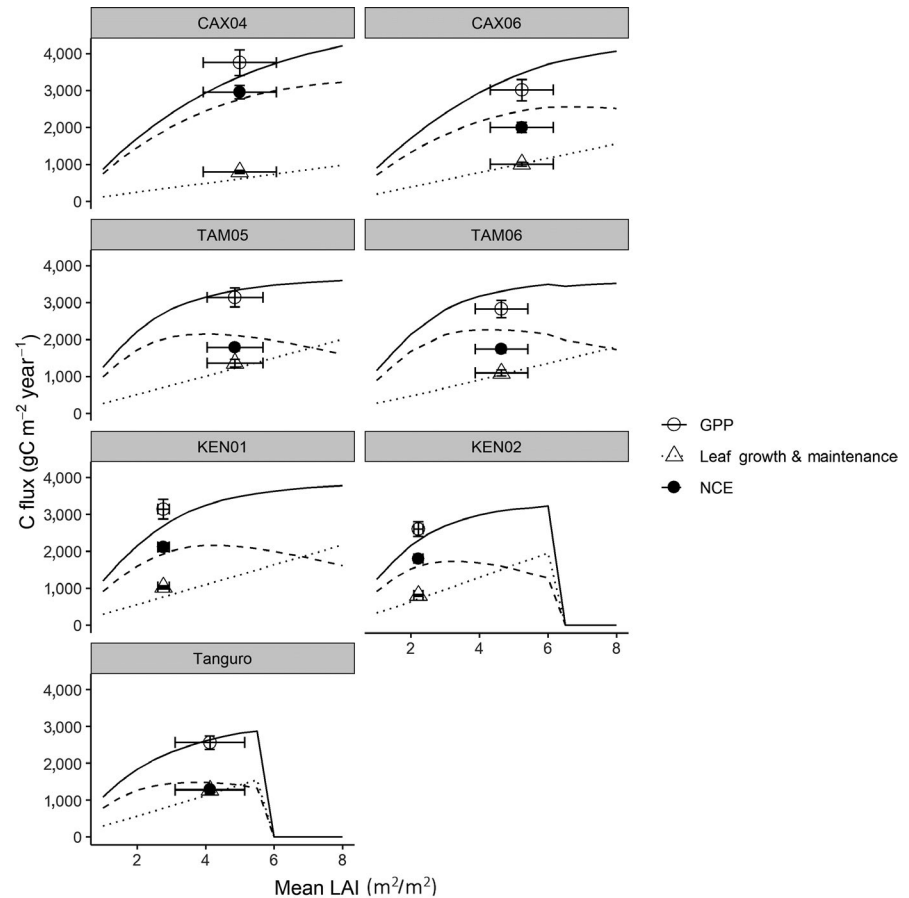
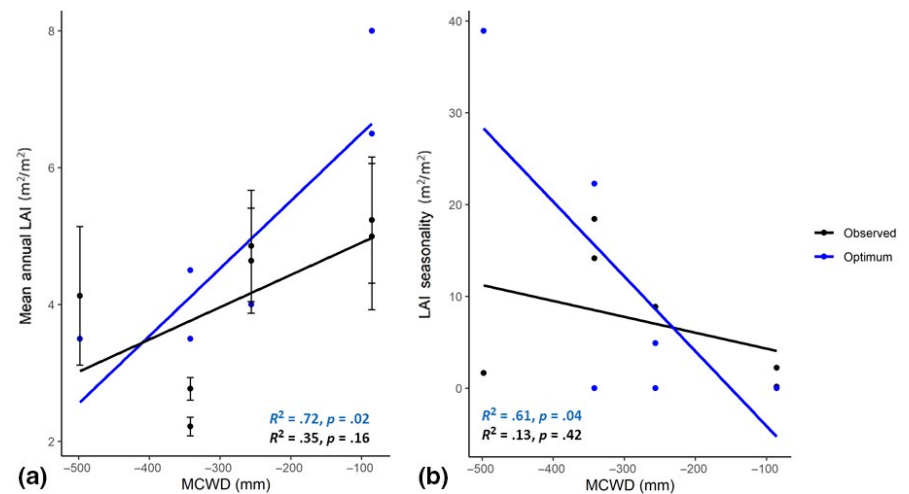


**FIGURE 5** The interaction between maximum climatological water deficit and simulated optimal (i.e. that which maximises net canopy C export) and observed (i.e. field-measured) mean annual leaf area index (LAI) (a) and LAI seasonality (b)



### 3.4 | Consistency between in situ LAI measurements and optimality-based predictions from mean LAI experiment

In situ measured LAI ( $\text{LAI}_{\text{field}}$ ) maximised NCE without matching predicted optimal mean LAI (Figure 5a). Field measurements of NCE correlated significantly with simulated optimal NCE ( $\text{NCE}_{\text{Opt}}$ ; Figure 6;  $R^2 = .83, p = .004$ ). Modelled NCE when SPA was forced with observed LAI was also consistent with  $\text{NCE}_{\text{Opt}}$  ( $R^2 = .94, p < .001$ ). Yet,

$\text{LAI}_{\text{field}}$  did not correlate significantly with simulated mean  $\text{LAI}_{\text{Opt}}$  ( $\text{mean LAI}_{\text{Opt}} \sim \text{LAI}_{\text{field}}, R^2 = .29, p = .21$ ). Across the moisture stress gradient, predicted mean  $\text{LAI}_{\text{Opt}}$  was 22.6% higher than  $\text{LAI}_{\text{field}}$ . Simulated mean  $\text{LAI}_{\text{Opt}}$  was within field observation error at three out of seven plots. In-situ measurements of LAI were simultaneously consistent with optimality-based predictions (i.e. maximised NCE), but inconsistent with predicted optimal LAI, because of the asymptotic response of simulated NCE to mean LAI over 1–2  $\text{m}^2/\text{m}^2$  differences in leaf cover (Figure 4).

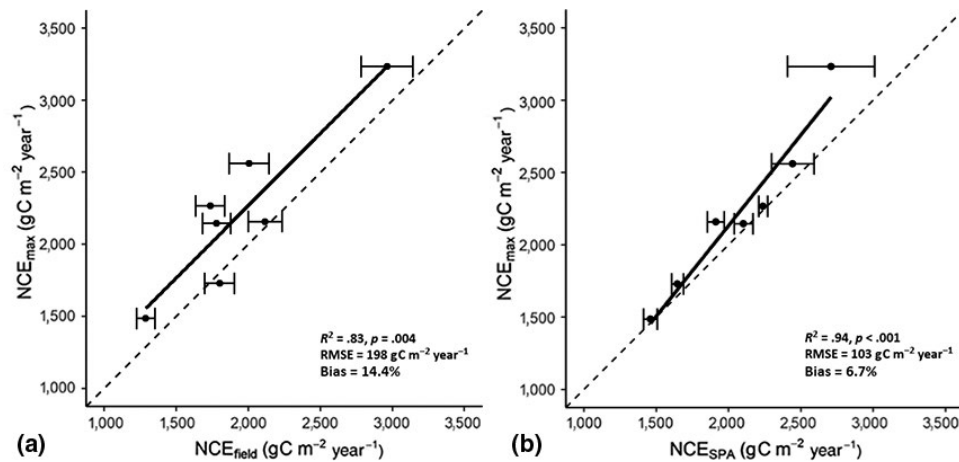


**FIGURE 6** A comparison of maximum simulated net canopy C export (NCE) forced with synthetic leaf area index (LAI) timeseries ranging in mean LAI against (a) field-estimated NCE, and (b) Soil-Plant-Atmosphere model (SPA) simulated NCE under nominal LAI. SPA error bars represent simulated NCE and gross primary productivity under field-measured LAI standard error. GEM error bars represent propagated error for summed field estimates of component net primary productivity and respiration. The dashed line is the 1:1 and the solid line is the linear regression between NCE estimates

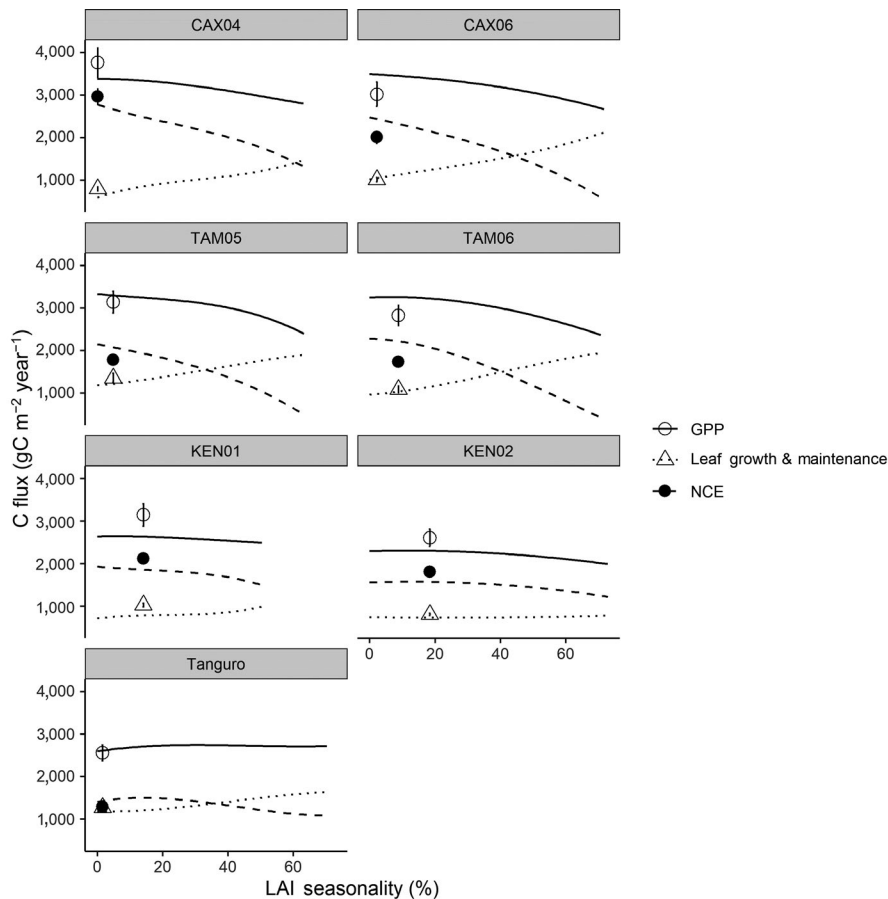


**FIGURE 7** Model-simulated net canopy C export (NCE), gross primary productivity (GPP) and leaf growth and maintenance, for each plot along an Amazon maximum climatological water deficit gradient, forced with synthetic leaf area index (LAI) timeseries ranging in LAI seasonality. Data points are field estimates of NCE, GPP and leaf growth and maintenance. Error bars show the propagated error of summed components

### 3.5 | Impact of LAI seasonality on NCE trade-offs across the soil moisture gradient

Trade-offs between leaf C costs and C assimilation resulted in seasonal LAI being deleterious within model simulations for forests occupying moister soils (Figure 6). However, for forests occupying drier

soils, a wide range of LAI seasonalities proved equally optimal. For forest plots occupying moister soils, simulated GPP declined with increasing LAI seasonality (Figure 7). For forest plots occupying drier soils, simulated GPP reached an asymptote across LAI seasonalities of between 0% and 40%, declining thereafter. Across all plots, the modelled C cost of leaf growth and maintenance increased with LAI

seasonality. However, the slope of the leaf C cost LAI seasonality interaction was reduced for drier plots. At low moisture stress, the response of leaf C costs and C assimilation to LAI seasonality caused simulated NCE to decline with increasing LAI seasonality. At high moisture stress, simulated NCE varied little across a range of LAI seasonalities before declining. As a result, simulated optimal LAI seasonality increased significantly with moisture stress ( $\text{LAI}_{\text{Opt}}$  seasonality  $\sim$  MCWD  $R^2 = .61$ ,  $p = .04$ ; Figure 5b).

### 3.6 | Consistency between in situ LAI measurements and optimality-based predictions from LAI seasonality experiment

Akin to trends in mean LAI, field-measured LAI seasonality maximised NCE, but did not match the predicted optimal LAI seasonality. Across the moisture stress gradient,  $\text{NCE}_{\text{field}}$  correlated significantly with predicted  $\text{NCE}_{\text{Opt}}$  ( $\text{NCE}_{\text{Opt}} \sim \text{NCE}_{\text{field}}$   $R^2 = .60$ ,  $p = .04$ ,  $\text{RMSE} = 257.5 \text{ gC m}^{-2} \text{ year}^{-1}$ ,  $\text{bias} = 6.5\%$ ). Modelled NCE when SPA was forced with observed LAI was also consistent with predicted  $\text{NCE}_{\text{Opt}}$  ( $\text{NCE}_{\text{Opt}} \sim \text{NCE}_{\text{SPA}}$   $R^2 = .98$ ,  $p < .001$ ,  $\text{RMSE} = 43.1 \text{ gC m}^{-2} \text{ year}^{-1}$ ,  $\text{bias} = 1.2\%$ ).  $\text{LAI}_{\text{field}}$  seasonality did not correlate significantly with simulated  $\text{LAI}_{\text{Opt}}$  seasonality ( $\text{LAI}_{\text{Opt}}$  seasonality  $\sim \text{LAI}_{\text{field}}$  seasonality  $R^2 = .08$ ,  $p = .5$ ). As before, field-measured LAI seasonality supported optimal NCE without matching the simulated optimal LAI seasonality, because of the asymptotic response of simulated NCE across a range of LAI seasonalities (Figure 7).

### 3.7 | Leaf trait interactions with the NCE along the soil moisture gradient

Slow leaf traits were optimal (i.e. maximised simulated NCE) under high mean LAI, while fast leaf traits were optimal under low mean LAI (Figure 8). Simulated  $\text{LAI}_{\text{Opt}}$  was  $2.5 \text{ m}^2/\text{m}^2$  higher under slow leaf traits compared to fast leaf traits, independent of moisture stress (Figure 8 upper panels). Under high moisture stress, slow leaf traits outperformed fast leaf traits (with respect to simulated NCE maximisation) for  $\text{LAI} > 4 \text{ m}^2/\text{m}^2$ . The transition point increased to  $\sim 5.5 \text{ m}^2/\text{m}^2$  under low moisture stress. When the model was forced with local, observed LAI at the low moisture stress plot, there was no significant difference in simulated NCE between nominal-slow and alternate fast leaf traits (nominal-slow  $2,709 \pm 301 \text{ gC m}^{-2} \text{ year}^{-1}$ ; alternate fast  $2,846 \pm 73 \text{ gC m}^{-2} \text{ year}^{-1}$ ). Under high moisture stress, when the model was forced with observed LAI, NCE was 33% higher for nominal-fast traits compared to alternate slow leaf traits (nominal-fast  $1,647 \pm 41 \text{ gC m}^{-2} \text{ year}^{-1}$ ; alternate slow  $1,238 \pm 57 \text{ gC m}^{-2} \text{ year}^{-1}$ ). The interaction between optimal leaf trait strategy and mean LAI matched the observed coordination between leaf and canopy properties across the moisture stress gradient.

Under high moisture stress, fast leaf traits were optimal across a range of LAI seasonalities (Figure 8). Under low moisture

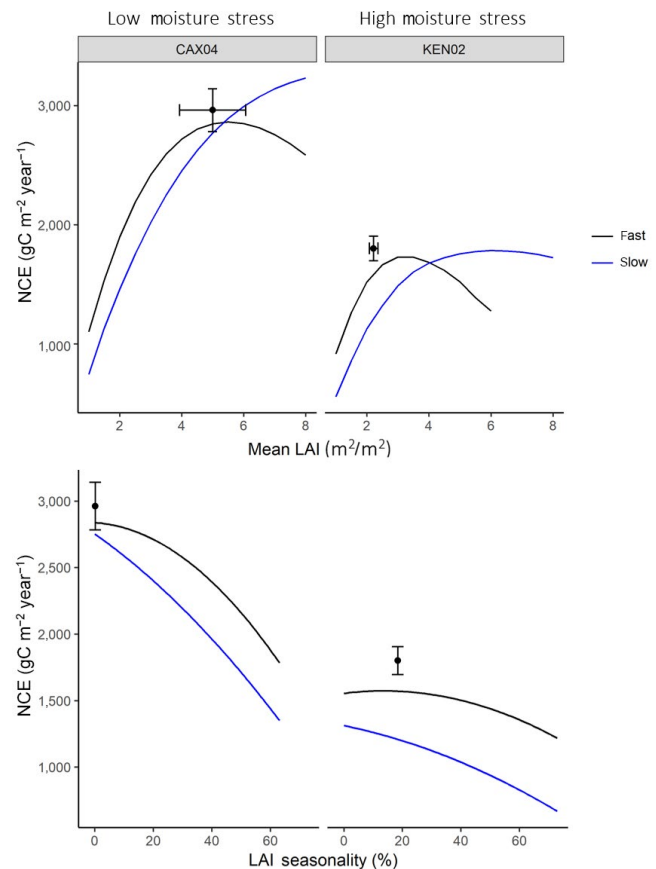


**FIGURE 8** Simulated net canopy C export (NCE) for Amazon forest plots under low (CAX04) and high (KEN02) moisture stress, forced with synthetic leaf area index (LAI) timeseries ranging in mean LAI (top panels) and LAI seasonality (bottom panels) under fast (black) and slow (blue) leaf traits. Data points are field estimates of mean LAI/LAI seasonality and NCE. Vertical error bars show the propagated error of summed components. Horizontal error bars show LAI standard error

stress, aseasonal LAI was optimal regardless of leaf trait strategy. At the drier forest plot, fast leaf traits generated stable simulated NCE across LAI seasonalities of 0%–25%, declining thereafter. At the moister forest plot, simulated NCE was maximised under aseasonal LAI; at 0% LAI seasonality under fast leaf traits; and at 0.17% LAI seasonality under slow leaf traits. Under high moisture stress, simulated  $\text{LAI}_{\text{Opt}}$  seasonality was 22% under fast leaf traits, which is close to  $\text{LAI}_{\text{field}}$  seasonality at 18%. Similarly, under low moisture stress, simulated  $\text{LAI}_{\text{Opt}}$  seasonality was 0.17% under slow leaf traits which matches observed  $\text{LAI}_{\text{field}}$  seasonality at 0.2%.

## 4 | DISCUSSION

Our aim was to test if key ecosystem properties (i.e. LAI dynamics and leaf trait suites) along a tropical forest MCWD gradient could be predicted using an optimality-based approach. We computed the sensitivity of NCE (representing C economic trade-offs,

i.e. C assimilation minus leaf growth and maintenance C costs) to moisture stress across a spectrum of LAI strategies using a detailed process based model of C uptake, allocation and turnover. As moisture stress increases, optimal mean LAI (i.e. that which maximised NCE) decreases, and optimal LAI seasonality increases. However, an asymptotic response of NCE to mean LAI and LAI seasonality limits the predictive power of an optimality-based approach (Figure 4); optimal LAI estimates do not match in-situ observations closely. We went further, to evaluate the sensitivity of C cycle dynamics to coincident variation in leaf traits, LAI and moisture stress. For forest plots occupying moister soils, slow leaf traits (i.e. long leaf lifespan, high LMA, low photosynthetic capacity and low metabolic rate) are optimal under aseasonal, high LAI. For forest plots occupying drier soils, fast leaf traits (i.e. short leaf lifespan, low LMA, high photosynthetic capacity and high metabolic rate) are optimal under low LAI (across LAI seasonalities of 0%–20%). Predicted optimal combinations of mean LAI, LAI seasonality and leaf traits reflect observed dynamics across the moisture stress gradient.

#### 4.1 | Divergence in canopy economics across the MCWD gradient drives optimal LAI

Model experiments indicated that at the drier end of the moisture gradient high LAI canopies are economically unfavourable (Figure 4). Any C gains (via photosynthesis) from additional leaf area are outweighed by the increase in leaf growth and maintenance C costs. Thus, consistent with our hypothesis, simulated NCE was maximised in drier forests by seasonal, low mean LAI (Figures 4 and 5). Under moister conditions, simulated NCE was maximised by aseasonal, high mean LAI. Photosynthetic gains are maintained with high LAI canopies, and are economical, as soil moisture is a less limiting factor.

#### 4.2 | Maximisation of NCE does not predict in-situ LAI

As hypothesised, in-situ LAI measurements maximise NCE and are therefore consistent with optimality-based predictions (Figure 6). Yet, simulated optimal LAI is a relatively poor predictor of observed LAI dynamics (Figure 5). Simulated NCE responds asymptotically to changes in LAI seasonality at drier plots (Figure 7), and mean LAI (Figure 4). For example, NCE can vary little across a mean LAI range of c.  $2 \text{ m}^2/\text{m}^2$  and a LAI seasonality range of up to 40% because of the complex trade-offs in the C economy linked to structural-functional interactions. This low sensitivity allows a range of mean LAI/LAI seasonalities to be similarly economically viable. As a result, despite matching optimality-based predictions (i.e. maximising NCE), mean  $\text{LAI}_{\text{field}}$  is not itself predicted well purely by the maximisation of NCE. Additional constraints to  $\text{LAI}_{\text{field}}$  beyond C economics are then under-determined.

Nutrient limitation was not accounted for in this analysis, but could be the additional constraint needed to improve optimality-based LAI predictions. Where moisture stress is low, but nutrients are limited (i.e. Caxiuanã), optimal LAI exceeds in-situ measurements (Figure 4). Kumagai et al. (2006) report higher LAIs of up to  $6.8 \text{ m}^2/\text{m}^2$  ( $\bar{x} = 6.2 \text{ m}^2/\text{m}^2$ ) in Bornean forests. Limited measurements indicate that soil N and pH across the Lambir Hills region are higher than at the Caxiuanã plots, as is soil phosphorus (CAX04 only; Davies et al., 2005; Malhi et al., 2015; Quesada et al., 2010). Furthermore, field evidence shows that total leaf litterfall is positively associated with soil richness (Chave et al., 2010), and thus soil nutrient availability is likely to have a determinate effect on LAI dynamics. We suggest that foliar N and P demands may preclude otherwise optimal, higher LAI, in nutrient poor forests.

Alternatively, the disparity between predicted optimal LAI and in-situ LAI measurements could be a result of a focus solely on foliar investment. One hypothesis is that returns on canopy investment could decline relative to returns from investing in other tissues which support leaf function; for example, investment in roots for nutrient acquisition (e.g. Thomas & Williams, 2014). The inclusion of investment returns across plant components could potentially reduce the range of equally viable LAI dynamics under current model assumptions. Haverd et al. (2016) have demonstrated optimisation of above versus belowground allocation to capture canopy dynamics across an Australian precipitation gradient. Another hypothesis is that LAI optimisation is sensitive to a reduction in marginal return rate (i.e. as the relative increase in net C gain starts to decline, plants may cease allocation towards the canopy). Further investigation into the presented model simulations show that if a marginal return rate function is added, whereby LAI ceases to increase when NCE is within  $<100 \text{ gC m}^{-2} \text{ year}^{-1}$  of the maximum, mean LAI is more successfully predicted ( $R^2 = .56$ ,  $p = .05$ , compared to simulated mean  $\text{LAI}_{\text{Opt}} \sim \text{LAI}_{\text{field}}$   $R^2 = .29$ ,  $p = .21$ ).

Differences between simulated optimal LAI and observed LAI could also result from the radiative transfer scheme used. Braghieri et al. (2019) recently found that the inclusion of leaf clumping into the radiative transfer scheme alleviated light limitation in lower canopy layers, especially where LAI was high (i.e. in the tropics). GPP increased as a result. However, leaf clumping was not simulated within SPA as local clumping estimates are unavailable for this study. Further work could therefore usefully test the sensitivity of NCE and LAI optimality to radiative transfer schemes.

With respect to LAI seasonality, the viability of both seasonal and aseasonal LAI at drier forest plots is ecologically consistent with the expectation that high climatic seasonality promotes the coexistence of different LAI strategies (i.e. deciduous-evergreen; Sakschewski et al., 2015). Furthermore, it is also consistent with in-situ observations. For example, at the Kenia plots, both deciduous (e.g. *Hura crepitans* L.) and evergreen (e.g. *Dendropanax arboreus*) species are present (Abelho et al., 2005; Figueroa-Esquivel et al., 2009; Poorter & Bongers, 2006). Given the interaction between LAI seasonality and leaf trait strategy, we might expect

community trait composition to also support a range of viable strategies (see Section 4.5).

### 4.3 | Should optimisation of whole stand C dynamics predict in situ LAI?

In addition to asking why optimisation of whole stand NCE does not predict observed LAI, we ask whether indeed it should (Anten & During, 2011). To date, optimality-based ecosystem models and DGVMs have had varied success in predicting mean and seasonal LAI values that are consistent with field observations (De Kauwe et al., 2014; McMurtrie et al., 2008; Thomas & Williams, 2014; Walker, Hanson, et al., 2014), and efforts have typically focused on single, mono-specific stands. In a mixed-species forest, where a variety of plant strategies co-exist, LAI which exceeds the forest-wide optimum would increase competitiveness in individual trees (Anten, 2016). van Loon et al. (2014) demonstrated how the inclusion of stem competition improved optimality-based predictions of LAI. However, given that in our study  $LAI_{\text{field}}$  was typically lower than simulated optimal LAI, including competition would not reduce the disparity between our optimality-based predictions and in-situ LAI measurements. Furthermore, the disparity between observed and simulated optimal LAI could be the result of our fitness proxy selection (Dewar et al., 2009). While NCE has proved a suitable measure of plant fitness elsewhere (McMurtrie & Dewar, 2011), it does not capture all aspects of plant fitness. It is possible that the appropriateness of NCE as a fitness proxy shifts as drought, nutrient limitation and disturbance increase, and plants must balance investment risk against shorter-term C gains.

### 4.4 | Leaf traits determine optimal LAI

Simulated optimal mean LAI is dependent on leaf traits. Within model experiments, independent of precipitation regime, fast leaf traits support low mean LAI, while slow leaf traits support high mean LAI (consistent with in-situ data; Figure 8; Table 2). As LAI increases, photosynthesis per unit leaf area declines. Consequently, under fast leaf traits, high respiratory C costs begin to outweigh C gains from high photosynthetic capacity. Conversely, lower respiratory C costs under slow leaf traits are sustainable as leaf area increases.

We show that leaf traits do not influence simulated optimal LAI seasonality at the moister forest plot where aseasonal LAI is most remunerative (Figure 8). However, at the drier forest plot, slow leaf traits are most remunerative under aseasonal LAI only, while fast leaf traits support a wider range of LAI seasonalities (0%–20%). Low leaf growth C costs and high photosynthetic capacity allow fast leaf traits to support different LAI seasonalities (though notably at low mean LAI). Slow leaf traits were unable to achieve the same viable range in LAI seasonality, as the increase in new leaf growth (following seasonal turnover) had a higher C cost (due to high LMA).

### 4.5 | Fast and slow leaf traits both maximise fitness in dry forest plots, but at different LAI

Model experiments, at drier forest plots, showed that fast and slow leaf trait strategies are equally viable, but at different mean LAI (Figure 8). These findings align with early conceptual approaches which used cost-benefit analyses to demonstrate how links between leaf longevity and phenology in temperate forests support coexistence of evergreen and deciduous trees (Kikuzawa, 1991, 1996). Reporting on dry tropical evergreen and deciduous forests in Cambodia, Ito et al. (2007) focused on sites located within 15 km which were thus assumed to be under the same precipitation regime. The evergreen forest had a mean LAI of  $4.05 \text{ m}^2/\text{m}^2$ , while the deciduous forest had a much lower mean LAI of  $0.88 \text{ m}^2/\text{m}^2$ . The difference in LAI is similar to that reported in this study, between predicted optimal LAI under slow and fast leaf traits at the dry forest plot ( $\sim 2.5 \text{ m}^2/\text{m}^2$ ). Our results are also consistent with that of Sakschewski et al. (2015), who predict that variability in plant strategies should be highest in drier, seasonal areas. Our findings suggest that trait trade-offs across the leaf economic spectrum offer alternative routes to viable strategies, supporting different forest types under similar climates.

### 4.6 | Leaf trait LAI dynamics are important to C cycling modelling

Our findings align with a growing body of evidence which demonstrates the major role of leaf trait LAI dynamics in driving regional to global scale variation in C fluxes (Trugman, et al., 2019; Trugman, et al., 2019; Verheijen et al., 2013; Xu et al., 2016). We therefore highlight the importance of concerted efforts to collate canopy aggregated leaf trait data (including LMA, photosynthetic rate, respiration rate and leaf lifespan) and to record these characteristics through the canopy profile and over full phenological cycles (Lloyd et al., 2010; Meir et al., 2002). Trait data need to be linked to LAI observations and scaled appropriately to understand their economic interactions and sensitivities.

### 4.7 | Limitations

We identify a number of limitations to our results including the absence of leaf age effects, the leaf respiration model used, uncertainty in LAI field estimates and lack of in situ data on the vertical profile of LAI within the canopy, except at a few tropical forest sites (Meir et al., 2000; Piayda et al., 2015). In addition, we recognise that by not including error associated with all model parameters, nor including model structural error, the C flux uncertainty values presented in our analysis are likely underestimated. In particular, our assumption of similar plant hydraulics across sites needs further exploration. These weaknesses can be addressed through concerted modelling and data collection exercises.

We do not simulate a leaf age effect on carboxylation and electron transport rates as to do so would have induced greater uncertainty



into our results. Wu et al. (2016) suggest that the interaction between leaf age and photosynthetic capacity reported for tropical forests (Kitajima et al., 1997, 2002; Xu et al., 2017), drives seasonal C flux dynamics. However, there were insufficient data currently to parameterise the leaf aging process across Amazon trees.

We recognise the limitations of the leaf maintenance respiration model used, namely that although based on biological reasoning, it is an empirical approach (scaling respiration from leaf N content as a function of temperature to estimate respiration), and that tropical trees accounted for only a small proportion of the data used to build the model (Reich et al., 2008). Other models relating leaf N content to respiration rate vary in their parameterisation and form (i.e. linear vs. the non-linear Reich model; Atkin et al., 2015; Meir et al., 2001; Ryan, 1991). It is vital to improve process modelling of autotrophic respiration, and to find ways to test scaling this leaf process to the canopy, and evaluate its climate sensitivity (Thomas et al., 2019).

While accounting for LAI sampling uncertainty in our results, there is a risk of measurement bias which could shift reported LAI trends, especially at higher leaf area (Bréda, 2003; Jonckheere et al., 2004; Weiss et al., 2004). However, our LAI estimates (from hemispherical photographs) align approximately with destructive sampling measurements from Amazon forests under a similar precipitation regime (Caxiuanã  $5.11 \pm 1.41 \text{ m}^2/\text{m}^2$ , McWilliam et al. (1993),  $5.7 \pm 0.5 \text{ m}^2/\text{m}^2$ ; Araújo et al., 2002; Fisher et al., 2007) so bias effects are unlikely to be large enough to influence our conclusions. In addition, we note that by using linear interpolation to scale monthly LAI estimates to daily values, we may have introduced some uncertainty into our results. However, we expect the effect to be minimal relative to the effect of in situ LAI estimate uncertainty.

The sensitivity of NCE to differences in the vertical distribution of LAI also remains uncertain. Within SPA, the default assumption is to uniformly distribute LAI over the canopy, as done here due to the lack of in-situ information. However, existing analysis of Amazonian forests have shown that the vertical profile of LAI can deviate significantly from a uniform distribution potentially resulting in significant changes in light absorption and leaf ecophysiological properties (Meir et al., 2000; Stark et al., 2012), as also found in temperate forests (Kull et al., 1999). Stark et al. (2012) compared ground-based and airborne Lidar estimation of vertical canopy profile of LAI, demonstrating the potential utility of airborne Lidar to resolve this current knowledge gap. An additional complication not yet addressed is that satellite and ground-based Lidar studies have presented evidence of divergent phenologies across different canopy layers (Smith et al., 2019; Tang & Dubayah, 2017).

## 5 | CONCLUSION

We assessed the potential for optimality-based approaches to improve predictions of tropical LAI and reduce uncertainty in C flux estimates. Our results show that LAI variation across an Amazon-wide

moisture stress gradient was optimal in terms of maximising NCE, but that the predictive power of this focused optimisation approach was limited with respect to LAI, as a range of LAI strategies could be equally economically viable. We also demonstrated how different leaf trait strategies can support alternative LAI dynamics. Given the importance of leaf traits in shaping canopy dynamics, we further highlight the importance of mapping spatial, temporal and vertical leaf trait distributions via databases (such as the TRY trait database) and new remote-sensing approaches.

## ACKNOWLEDGEMENTS

The authors would like to thank the PhD project funding body, the UK Natural Environment Research Council E3 DTP, NERC, the GHG program GREENHOUSE (NE/K002619/1), the UK's National Centre for Earth Observation (NE/R016518/1), the UKSA project Forests 2020, a Royal Society Wolfson Award to M.W., the UK Met Office, the Newton Fund and the CSSP-Brazil project. P.M. also acknowledges support from NERC grant NE/J011002/1 and ARC grant DP170104091. The TRY trait database is thanked for the data used in model parameterisation and the authors would like to thank the Global Ecosystems Monitoring network team for the field data used in this study, collected through funding from NERC and the Gordon and Betty Moore Foundation, and an ERC Advanced Investigator Award to Y.M. (GEM-TRAIT). In addition, the authors would like to thank the anonymous reviewers for their constructive feedback on the manuscript.

## CONFLICT OF INTEREST

The authors state no conflict of interest.

## AUTHOR CONTRIBUTION

S.F.-P., M.W. and P.M. conceived the research questions. Data used in model calibration and evaluation were collected by Y.M. and associates. Model experiments were designed and conducted by S.F.-P. with contributions from M.W. and T.L.S. S.F.-P. and M.W. prepared the manuscript with active contributions from all co-authors.

## DATA AVAILABILITY STATEMENT

The data that support the findings of this study are openly available in Edinburgh DataShare at <https://doi.org/10.7488/ds/2925>, reference number 10283/3761.

## ORCID

Sophie Flack-Prain  <https://orcid.org/0000-0003-0711-5057>

## REFERENCES

- Abelho, M., Cressa, C., & MaS, G. (2005). Microbial biomass, respiration, and decomposition of *Hura crepitans* L. (Euphorbiaceae) leaves in a tropical stream. *Biotropica*, 37, 397–402. <https://doi.org/10.1111/j.1744-7429.2005.00052.x>
- Ackerly, D. (1999). Self-shading, carbon gain and leaf dynamics: A test of alternative optimality models. *Oecologia*, 119, 300–310. <https://doi.org/10.1007/s004420050790>

- Amthor, J. S., Goulden, M. L., Munger, J. W., & Wofsy, S. C. (1994). Testing a mechanistic model of forest-canopy mass and energy exchange using eddy correlation: Carbon dioxide and ozone uptake by a mixed oak-maple stand. *Functional Plant Biology*, 21, 623–651. <https://doi.org/10.1071/PP9940623>
- Anten, N. P. R. (2016). Optimization and game theory in canopy models. *Canopy photosynthesis: From basics to applications* (pp. 355–377). Springer. [https://doi.org/10.1007/978-94-017-7291-4\\_13](https://doi.org/10.1007/978-94-017-7291-4_13)
- Anten, N. P. R., & During, H. J. (2011). Is analysing the nitrogen use at the plant canopy level a matter of choosing the right optimization criterion? *Oecologia*, 167, 293–303. <https://doi.org/10.1007/s00442-011-2011-3>
- Aragao, L. E. O. C., Malhi, Y., Metcalfe, D. B., Silva-Espejo, J. E., Jimenez, E., Navarrete, D., Almeida, S., Costa, A. C. L., Salinas, N., Phillips, O. L., Anderson, L. O., Alvarez, E., Baker, T. R., Goncalves, P. H., Huaman-Ovalle, J., Mamani-Solorzano, M., Meir, P., Monteagudo, A., Patino, S., ... Vasquez, R. (2009). Above- and below-ground net primary productivity across ten Amazonian forests on contrasting soils. *Biogeosciences*, 6, 2759–2778. <https://doi.org/10.5194/bg-6-2759-2009>
- Araújo, A. C., Nobre, A. D., Kruijt, B., Elbers, J. A., Dallarosa, R., Stefani, P., Von Randow, C., Manzi, A. O., Culf, A. D., & Gash, J. H. C. (2002). Comparative measurements of carbon dioxide fluxes from two nearby towers in a central Amazonian rainforest: The Manaus LBA site. *Journal of Geophysical Research: Atmospheres*, 107, LBA-58. <https://doi.org/10.1029/2001JD000676>
- Araujo-Murakami, A., Doughty, C. E., Metcalfe, D. B., Silva-Espejo, J. E., Arroyo, L., Heredia, J. P., Flores, M., Sibling, R., Mendizabal, L. M., Pardo-Toledo, E., Vega, M., Moreno, L., Rojas-Landivar, V. D., Halladay, K., Caj, G., Killeen, T. J., & Malhi, Y. (2014). The productivity, allocation and cycling of carbon in forests at the dry margin of the Amazon forest in Bolivia. *Plant Ecology & Diversity*, 7, 55–69. <https://doi.org/10.1080/17550874.2013.798364>
- Atkin, O. K., Bloomfield, K. J., Reich, P. B., Tjoelker, M. G., Asner, G. P., Bonal, D., Bönsch, G., Bradford, M. G., Cernusak, L. A., Cosio, E. G., Creek, D., Crous, K. Y., Domingues, T. F., Dukes, J. S., Egerton, J. J. G., Evans, J. R., Farquhar, G. D., Fyllas, N. M., Gauthier, P. P. G., ... Zaragoza-Castells, J. (2015). Global variability in leaf respiration in relation to climate, plant functional types and leaf traits. *New Phytologist*, 206, 614–636. <https://doi.org/10.1111/nph.13253>
- Baldocchi, D., Valentini, R., Running, S., Oechel, W., & Dahlman, R. (1996). Strategies for measuring and modelling carbon dioxide and water vapour fluxes over terrestrial ecosystems. *Global Change Biology*, 2, 159–168. <https://doi.org/10.1111/j.1365-2486.1996.tb00069.x>
- Bloom, A. A., & Williams, M. (2015). Constraining ecosystem carbon dynamics in a data-limited world: Integrating ecological "common sense" in a model-data fusion framework. *Biogeosciences*, 12, 1299–1315. <https://doi.org/10.5194/bg-12-1299-2015>
- Bonan, G. B., Williams, M., Fisher, R. A., & Oleson, K. W. (2014). Modeling stomatal conductance in the earth system: Linking leaf water-use efficiency and water transport along the soil-plant-atmosphere continuum. *Geoscientific Model Development*, 7, 2193–2222. <https://doi.org/10.5194/gmd-7-3085-2014>
- Braghiere, R. K., Quafe, T., Black, E., He, L., & Chen, J. M. (2019). Underestimation of global photosynthesis in Earth System Models due to representation of vegetation structure. *Global Biogeochemical Cycles*, 33, 1358–1369. <https://doi.org/10.1029/2018GB006135>
- Bréda, N. J. J. (2003). Ground-based measurements of leaf area index: A review of methods, instruments and current controversies. *Journal of Experimental Botany*, 54, 2403–2417. <https://doi.org/10.1093/jxb/erg263>
- Caldararu, S., Palmer, P. I., & Purves, D. W. (2012). Inferring Amazon leaf demography from satellite observations of leaf area index. *Biogeosciences*, 9, 1389–1404. <https://doi.org/10.5194/bg-9-1389-2012>
- Caldararu, S., Purves, D. W., & Palmer, P. I. (2014). Phenology as a strategy for carbon optimality: A global model. *Biogeosciences*, 11, 763–778. <https://doi.org/10.5194/bg-11-763-2014>
- Caldararu, S., Purves, D. W., & Smith, M. J. (2016). The effect of using the plant functional type paradigm on a data-constrained global phenology model. *Biogeosciences*, 13, 925–941. <https://doi.org/10.5194/bg-13-925-2016>
- Carswell, F. E., Costa, A. L., Palheta, M., Malhi, Y., Meir, P., Costa, J. D. R., Ruivo, M. D., Leal, L. D. M., Costa, J. M. N., Clement, R. J., & Grace, J. (2002). Seasonality in CO<sub>2</sub> and H<sub>2</sub>O flux at an eastern Amazonian rain forest. *Journal of Geophysical Research-Atmospheres*, 107. <https://doi.org/10.1029/2000JD000284>
- Carswell, F. E., Meir, P., Wandelli, E. V., Bonates, L. C. M., Kruijt, B., Barbosa, E. M., Nobre, A. D., Grace, J., & Jarvis, P. G. (2000). Photosynthetic capacity in a central Amazonian rain forest. *Tree Physiology*, 20, 179–186. <https://doi.org/10.1093/treephys/20.3.179>
- Chave, J., Navarrete, D., Almeida, S., Álvarez, E., Aragão, L. E. O. C., Bonal, D., Châtelet, P., Silva-Espejo, J. E., Goret, J.-Y., von Hildebrand, P., Jiménez, E., Patiño, S., Peñuela, M. C., Phillips, O. L., Stevenson, P., & Malhi, Y. (2010). Regional and seasonal patterns of litterfall in tropical South America. *Biogeosciences*, 7, 43–55. <https://doi.org/10.5194/bg-7-43-2010>
- Clark, D. B., Mercado, L. M., Sitch, S., Jones, C. D., Gedney, N., Best, M. J., Pryor, M., Rooney, G. G., Essery, R. L. H., Blyth, E., Boucher, O., Harding, R. J., Huntingford, C., & Cox, P. M. (2011). The Joint UK Land Environment Simulator (JULES), model description – Part 2: Carbon fluxes and vegetation dynamics. *Geoscientific Model Development*, 4, 701–722. <https://doi.org/10.5194/gmd-4-701-2011>
- Davies, S. J., Tan, S., Lafrankie, J. V., & Potts, M. D. (2005). Soil-related floristic variation in a hyperdiverse dipterocarp forest. In D. W. Roubik, S. Sakai, & A. A. Karim (Eds.), *Pollination ecology and the rain forest*. Ecological Studies (Analysis and Synthesis) (Vol. 174, pp. 22–34). Springer. [https://doi.org/10.1007/0-387-27161-9\\_3](https://doi.org/10.1007/0-387-27161-9_3)
- De Kauwe, M. G., Medlyn, B. E., Zaehle, S., Walker, A. P., Dietze, M. C., Wang, Y. P., Luo, Y., Jain, A. K., El-Masri, B., & Hickler, T. (2014). Where does the carbon go? A model-data intercomparison of vegetation carbon allocation and turnover processes at two temperate forest free-air CO<sub>2</sub> enrichment sites. *New Phytologist*, 203, 883–899. <https://doi.org/10.1111/nph.12847>
- De Weirtd, M., Verbeeck, H., Maignan, F., Peylin, P., Poulter, B., Bonal, D., Ciais, P., & Steppe, K. (2012). Seasonal leaf dynamics for tropical evergreen forests in a process-based global ecosystem model. *Geoscientific Model Development*, 5, 1091–1108. <https://doi.org/10.5194/gmd-5-1091-2012>
- Dee, D. P., Uppala, S. M., Simmons, A. J., Berrisford, P., Poli, P., Kobayashi, S., Andrae, U., Balmaseda, M. A., Balsamo, G., Bauer, P., Bechtold, P., Beljaars, A. C. M., van de Berg, L., Bidlot, J., Bormann, N., Delsol, C., Dragani, R., Fuentes, M., Geer, A. J., ... Vitart, F. (2011). The ERA-Interim reanalysis: Configuration and performance of the data assimilation system. *Quarterly Journal of the Royal Meteorological Society*, 137, 553–597. <https://doi.org/10.1002/qj.828>
- Dewar, R. C., Franklin, O., Mäkelä, A., Mcmurtrie, R. E., & Valentine, H. T. (2009). Optimal function explains forest responses to global change. *BioScience*, 59, 127–139. <https://doi.org/10.1525/bio.2009.59.2.6>
- Doughty, C. E., Metcalfe, D. B., Girardin, C. A., Amezquita, F. F., Cabrera, D. G., Huasco, W. H., Silva-Espejo, J. E., Araujo-Murakami, A., Da Costa, M. C., Rocha, W., Feldpausch, T. R., Mendoza, A. L., Da Costa, A. C., Meir, P., Phillips, O. L., & Malhi, Y. (2015). Drought impact on forest carbon dynamics and fluxes in Amazonia. *Nature*, 519, 78–82. <https://doi.org/10.1038/nature14213>
- Evans, J. R. (1989). Photosynthesis and nitrogen relationships in leaves of C3 plants. *Oecologia*, 78, 9–19. <https://doi.org/10.1007/BF00377192>
- Farquhar, G. D., & Von Caemmerer, S. (1982). Modelling of photosynthetic response to environmental conditions. *Physiological plant*

- ecology* II (pp. 549–587). Springer. [https://doi.org/10.1007/978-3-642-68150-9\\_17](https://doi.org/10.1007/978-3-642-68150-9_17)
- Field, C. (1983). Allocating leaf nitrogen for the maximization of carbon gain: Leaf age as a control on the allocation program. *Oecologia*, 56, 341–347. <https://doi.org/10.1007/BF00379710>
- Figuerola-Esquivel, E., Puebla-Olivares, F., Godínez-Álvarez, H., & Núñez-Farfán, J. (2009). Seed dispersal effectiveness by understory birds on *Dendropanax arboreus* in a fragmented landscape. *Biodiversity and Conservation*, 18, 3357–3365. <https://doi.org/10.1007/s10531-009-9645-z>
- Fisher, J. B., Badgley, G., & Blyth, E. (2012). Global nutrient limitation in terrestrial vegetation. *Global Biogeochemical Cycles*, 26, 3. <https://doi.org/10.1029/2011GB004252>
- Fisher, R. A., Williams, M., Da Costa, A. L., Malhi, Y., Da Costa, R. F., Almeida, S., & Meir, P. (2007). The response of an Eastern Amazonian rain forest to drought stress: Results and modelling analyses from a throughfall exclusion experiment. *Global Change Biology*, 13, 2361–2378. <https://doi.org/10.1111/j.1365-2486.2007.01417.x>
- Fisher, R. A., Williams, M., Do, V., Lobo, R., Da Costa, A. L., & Meir, P. (2006). Evidence from Amazonian forests is consistent with isohydric control of leaf water potential. *Plant, Cell & Environment*, 29, 151–165. <https://doi.org/10.1111/j.1365-3040.2005.01407.x>
- Flack-Prain, S., Meir, P., Malhi, Y., Smallman, T. L., & Williams, M. (2019). The importance of physiological, structural and trait responses to drought stress in driving spatial and temporal variation in GPP across Amazon forests. *Biogeosciences*, 16, 4463–4484. <https://doi.org/10.5194/bg-16-4463-2019>
- Franklin, O., Mcmurtrie, R., Iversen, C. M., Crous, K. Y., Finzi, A. C., Tissue, D. T., Ellsworth, D. S., RaM, O., & Norby, R. J. (2009). Forest fine-root production and nitrogen use under elevated CO<sub>2</sub>: Contrasting responses in evergreen and deciduous trees explained by a common principle. *Global Change Biology*, 15, 132–144. <https://doi.org/10.1111/j.1365-2486.2008.01710.x>
- Fyllas, N. M., Patino, S., Baker, T. R., Nardoto, G. B., Martinelli, L. A., Quesada, C. A., Paiva, R., Schwarz, M., Horna, V., Mercado, L. M., Santos, A., Arroyo, L., Jimenez, E. M., Luizao, F. J., Neill, D. A., Silva, N., Prieto, A., Rudas, A., Silveira, M., ... Lloyd, J. (2009). Basin-wide variations in foliar properties of Amazonian forest: Phylogeny, soils and climate. *Biogeosciences*, 6, 2677–2708. <https://doi.org/10.5194/bg-6-2677-2009>
- Geber, M. A., & Griffen, L. R. (2003). Inheritance and natural selection on functional traits. *International Journal of Plant Sciences*, 164, S21–S42. <https://doi.org/10.1086/368233>
- Givnish, T. J. (2002). Adaptive significance of evergreen vs. deciduous leaves: Solving the triple paradox. *Silva Fennica*, 36, 703–743. <https://doi.org/10.14214/sf.535>
- Grier, C. C., & Running, S. W. (1977). Leaf area of mature northwestern coniferous forests – Relation to site water-balance. *Ecology*, 58, 893–899. <https://doi.org/10.2307/1936225>
- Haverd, V., Smith, B., Raupach, M. R., Briggs, P. R., Nieradzik, L. P., Beringer, J., Hutley, L. B., Trudinger, C. M., & Cleverly, J. (2016). Coupling carbon allocation with leaf and root phenology predicts tree-grass partitioning along a savanna rainfall gradient. *Biogeosciences*, 13(3), 761–779. <https://doi.org/10.5194/bg-13-761-2016>
- Iio, A., Hikosaka, K., Anten, N. P. R., Nakagawa, Y., & Ito, A. (2014). Global dependence of field-observed leaf area index in woody species on climate: A systematic review. *Global Ecology and Biogeography*, 23, 274–285. <https://doi.org/10.1111/geb.12133>
- Ito, E., Khorn, S., Lim, S., Pol, S., Tith, B., Pith, P., Tani, A., Kanzaki, M., Kaneko, T., Okuda, Y., Kabeya, N., Nobuhiro, T., & Araki, M. (2007). Comparison of the leaf area index (LAI) of two types of dipterocarp forest on the west bank of the Mekong River, Cambodia. In H. Sawada, M. Araki, N. A. Chappell, J. V. Lafrankie, & A. Shimizu (Eds.), *Forest environments in the Mekong River Basin* (pp. 214–221). Springer. [https://doi.org/10.1007/978-4-431-46503-4\\_19](https://doi.org/10.1007/978-4-431-46503-4_19)
- Jolly, W. M., Nemani, R., & Running, S. W. (2005). A generalized, bioclimatic index to predict foliar phenology in response to climate. *Global Change Biology*, 11, 619–632. <https://doi.org/10.1111/j.1365-2486.2005.00930.x>
- Jonckheere, I., Fleck, S., Nackaerts, K., Muys, B., Coppin, P., Weiss, M., & Baret, F. (2004). Review of methods for in situ leaf area index determination – Part I. Theories, sensors and hemispherical photography. *Agricultural and Forest Meteorology*, 121, 19–35. <https://doi.org/10.1016/j.agrformet.2003.08.027>
- Kikuzawa, K. (1991). A cost-benefit analysis of leaf habit and leaf longevity of trees and their geographical pattern. *The American Naturalist*, 138, 1250–1263. <https://doi.org/10.1086/285281>
- Kikuzawa, K. (1996). Geographical distribution of leaf life span and species diversity of trees simulated by a leaf-longevity model. *Vegetation*, 122, 61–67. <https://doi.org/10.1007/BF00052816>
- Kim, Y., Knox, R. G., Longo, M., Medvigy, D., Hutya, L. R., Pyle, E. H., Wofsy, S. C., Bras, R. L., & Moorcroft, P. R. (2012). Seasonal carbon dynamics and water fluxes in an Amazon rainforest. *Global Change Biology*, 18, 1322–1334. <https://doi.org/10.1111/j.1365-2486.2011.02629.x>
- Kitajima, K., Mulkey, S. S., Samaniego, M., & Joseph Wright, S. (2002). Decline of photosynthetic capacity with leaf age and position in two tropical pioneer tree species. *American Journal of Botany*, 89, 1925–1932. <https://doi.org/10.3732/ajb.89.12.1925>
- Kitajima, K., Mulkey, S. S., & Wright, S. J. (1997). Decline of photosynthetic capacity with leaf age in relation to leaf longevities for five tropical canopy tree species. *American Journal of Botany*, 84, 702–708. <https://doi.org/10.2307/2445906>
- Kull, O., Broadmeadow, M., Kruijt, B., & Meir, P. (1999). Light distribution and foliage structure in an oak canopy. *Trees*, 14, 55–64. <https://doi.org/10.1007/s004680050209>
- Kumagai, T., Ichie, T., Yoshimura, M., Yamashita, M., Kenzo, T., Saitoh, T. M., Ohashi, M., Suzuki, M., Koike, T., & Komatsu, H. (2006). Modeling CO<sub>2</sub> exchange over a Bornean tropical rain forest using measured vertical and horizontal variations in leaf-level physiological parameters and leaf area densities. *Journal of Geophysical Research: Atmospheres*, 111, D10. <https://doi.org/10.1029/2005JD006676>
- Liu, J., Bowman, K. W., Schimel, D. S., Parazoo, N. C., Jiang, Z., Lee, M., Bloom, A. A., Wunch, D., Frankenberg, C., Sun, Y., O'Dell, C. W., Gurney, K. R., Menemenlis, D., Gierach, M., Crisp, D., & Eldering, A. (2017). Contrasting carbon cycle responses of the tropical continents to the 2015–2016 El Niño. *Science*, 358, 6360. <https://doi.org/10.1126/science.aam5690>
- Liu, Y., Xiao, J., Ju, W., Zhu, G., Wu, X., Fan, W., Li, D., & Zhou, Y. (2018). Satellite-derived LAI products exhibit large discrepancies and can lead to substantial uncertainty in simulated carbon and water fluxes. *Remote Sensing of Environment*, 206, 174–188. <https://doi.org/10.1016/j.rse.2017.12.024>
- Lloyd, J., Patiño, S., Paiva, R. Q., Nardoto, G. B., Quesada, C. A., Santos, A. J. B., Baker, T. R., Brand, W. A., Hilke, I., Gielmann, H., Raessler, M., Luizão, F. J., Martinelli, L. A., & Mercado, L. M. (2010). Optimisation of photosynthetic carbon gain and within-canopy gradients of associated foliar traits for Amazon forest trees. *Biogeosciences*, 7, 1833–1859. <https://doi.org/10.5194/bg-7-1833-2010>
- López-Blanco, E., Lund, M., Christensen, T. R., Tamstorf, M. P., Smallman, T. L., Slevin, D., Westergaard-Nielsen, A., Hansen, B. U., Abermann, J., & Williams, M. (2018). Plant traits are key determinants in buffering the meteorological sensitivity of net carbon exchanges of Arctic tundra. *Journal of Geophysical Research: Biogeosciences*, 123(9), 2675–2694. <https://doi.org/10.1029/2018JG004386>
- Malhi, Y., Amezquita, F. F., Doughty, C. E., Silva-Espejo, J. E., CaJ, G., Metcalfe, D. B., Aragao, L. E. O. C., Huaraca-Quispe, L. P., Alzamora-Taype, I., Eguiluz-Mora, L., Marthews, T. R., Halladay, K., Quesada, C. A., Robertson, A. L., Fisher, J. B., Zaragoza-Castells, J., Rojas-Villagra, C. M., Pelaez-Tapia, Y., Salinas, N., ... Phillips, O. L. (2014). The productivity, metabolism and carbon cycle of two lowland tropical forest

- plots in south-western Amazonia, Peru. *Plant Ecology & Diversity*, 7, 85–105. <https://doi.org/10.1080/17550874.2013.820805>
- Malhi, Y., Doughty, C. E., Goldsmith, G. R., Metcalfe, D. B., CaJ, G., Matthews, T. R., Del Aguila-Pasquel, J., Aragao, L. E. O. C., Araujo-Murakami, A., Brando, P., Da Costa, A. C. L., Silva-Espejo, J. E., Amezquita, F. F., Galbraith, D. R., Quesada, C. A., Rocha, W., Salinas-Revilla, N., Silverio, D., Meir, P., & Phillips, O. L. (2015). The linkages between photosynthesis, productivity, growth and biomass in lowland Amazonian forests. *Global Change Biology*, 21, 2283–2295. <https://doi.org/10.1111/gcb.12859>
- Malhi, Y., Roberts, J. T., Betts, R. A., Killeen, T. J., Li, W., & Nobre, C. A. (2008). Climate change, deforestation, and the fate of the Amazon. *Science*, 319, 169–172. <https://doi.org/10.1126/science.1146961>
- Mcmurtrie, R. E., & Dewar, R. C. (2011). Leaf-trait variation explained by the hypothesis that plants maximize their canopy carbon export over the lifespan of leaves. *Tree Physiology*, 31, 1007–1023. <https://doi.org/10.1093/treephys/tp037>
- Mcmurtrie, R. E., Norby, R. J., Medlyn, B. E., Dewar, R. C., Pepper, D. A., Reich, P. B., & Barton, C. V. M. (2008). Why is plant-growth response to elevated CO<sub>2</sub> amplified when water is limiting, but reduced when nitrogen is limiting? A growth-optimisation hypothesis. *Functional Plant Biology*, 35, 521–534. <https://doi.org/10.1071/FP08128>
- Mcwilliam, A. L., Roberts, J. M., Cabral, O. M. R., Leitao, M., De Costa, A. C. L., Maitelli, G. T., & Zamparoni, C. (1993). Leaf area index and above-ground biomass of terra firme rain forest and adjacent clearings in Amazonia. *Functional Ecology*, 7(3), 310–317. <https://doi.org/10.2307/2390210>
- Meir, P., Grace, J., & Miranda, A. C. (2000). Photographic method to measure the vertical distribution of leaf area density in forests. *Agricultural and Forest Meteorology*, 102, 105–111. [https://doi.org/10.1016/S0168-1923\(00\)00122-2](https://doi.org/10.1016/S0168-1923(00)00122-2)
- Meir, P., Grace, J., & Miranda, A. C. (2001). Leaf respiration in two tropical rainforests: Constraints on physiology by phosphorus, nitrogen and temperature. *Functional Ecology*, 15, 378–387. <https://doi.org/10.1046/j.1365-2435.2001.00534.x>
- Meir, P., Kruijt, B., Broadmeadow, M., Barbosa, E., Kull, O., Carswell, F., Nobre, A., & Jarvis, P. G. (2002). Acclimation of photosynthetic capacity to irradiance in tree canopies in relation to leaf nitrogen concentration and leaf mass per unit area. *Plant, Cell & Environment*, 25, 343–357. <https://doi.org/10.1046/j.0016-8025.2001.00811.x>
- Metcalfe, D. B., Meir, P., Aragão, L. E. O. C., Lobo-do-Vale, R., Galbraith, D., Fisher, R. A., Chaves, M. M., Maroco, J. P., da Costa, A. C. L., de Almeida, S. S., Braga, A. P., Gonçalves, P. H. L., de Athaydes, J., da Costa, M., Portela, T. T. B., ... Williams, M. (2010). Shifts in plant respiration and carbon use efficiency at a large-scale drought experiment in the eastern Amazon. *New Phytologist*, 187, 608–621. <https://doi.org/10.1111/j.1469-8137.2010.03319.x>
- Muraoka, H., Saigusa, N., Nasahara, K. N., Noda, H., Yoshino, J., Saitoh, T. M., Nagai, S., Murayama, S., & Koizumi, H. (2010). Effects of seasonal and interannual variations in leaf photosynthesis and canopy leaf area index on gross primary production of a cool-temperate deciduous broadleaf forest in Takayama, Japan. *Journal of Plant Research*, 123, 563–576. <https://doi.org/10.1007/s10265-009-0270-4>
- Myneri, R. B., Yang, W., Nemani, R. R., Huete, A. R., Dickinson, R. E., Knyazikhin, Y., Didan, K., Fu, R., Negrón Juárez, R. I., Saatchi, S. S., Hashimoto, H., Ichii, K., Shabanov, N. V., Tan, B., Ratana, P., Privette, J. L., Morissette, J. T., Vermote, E. F., Roy, D. P., ... Salomonson, V. V. (2007). Large seasonal swings in leaf area of Amazon rainforests. *Proceedings of the National Academy of Sciences of the United States of America*, 104, 4820–4823. <https://doi.org/10.1073/pnas.061138104>
- Osnas, J. L. D., Lichstein, J. W., Reich, P. B., & Pacala, P. W. (2013). Global leaf trait relationships: Mass, area, and the leaf economics spectrum. *Science*, 340(6133), 741–744. <https://doi.org/10.1126/science.1231574>
- Pan, Y., Birdsey, R. A., Fang, J., Houghton, R., Kauppi, P. E., Kurz, W. A., Phillips, O. L., Shvidenko, A., Lewis, S. L., Canadell, J. G., Ciais, P., Jackson, R. B., Pacala, S. W., McGuire, A. D., Piao, S., Rautiainen, A., Sitch, S., & Hayes, D. (2011). A large and persistent carbon sink in the world's forests. *Science*, 333, 988–993. <https://doi.org/10.1126/science.1201609>
- Piayda, A., Dubbert, M., Werner, C., Correia, A. V., Pereira, J. S., & Cuntz, M. (2015). Influence of woody tissue and leaf clumping on vertically resolved leaf area index and angular gap probability estimates. *Forest Ecology and Management*, 340, 103–113. <https://doi.org/10.1016/j.foreco.2014.12.026>
- Poorter, L., & Bongers, F. (2006). Leaf traits are good predictors of plant performance across 53 rain forest species. *Ecology*, 87, 1733–1743. [https://doi.org/10.1890/0012-9658\(2006\)87\[1733:LTAGPO\]2.0.CO;2](https://doi.org/10.1890/0012-9658(2006)87[1733:LTAGPO]2.0.CO;2)
- Quesada, C. A., Lloyd, J., Schwarz, M., Patino, S., Baker, T. R., Czimczik, C., Fyllas, N. M., Martinelli, L., Nardoto, G. B., Schmerler, J., Santos, A. J. B., Hodnett, M. G., Herrera, R., Luizao, F. J., Arneith, A., Lloyd, G., Dezzee, N., Hilke, I., Kuhlmann, I., ... Paiva, R. (2010). Variations in chemical and physical properties of Amazon forest soils in relation to their genesis. *Biogeosciences*, 7, 1515–1541. <https://doi.org/10.5194/bg-7-1515-2010>
- Quesada, C. A., Phillips, O. L., Schwarz, M., Czimczik, C. I., Baker, T. R., Patino, S., Fyllas, N. M., Hodnett, M. G., Herrera, R., Almeida, S., Davila, E. A., Arneith, A., Arroyo, L., Chao, K. J., Dezzee, N., Erwin, T., Di Fiore, A., Higuchi, N., Coronado, E. H., ... Lloyd, J. (2012). Basin-wide variations in Amazon forest structure and function are mediated by both soils and climate. *Biogeosciences*, 9, 2203–2246. <https://doi.org/10.5194/bg-9-2203-2012>
- Reich, P. B., Falster, D. S., Ellsworth, D. S., Wright, I. J., Westoby, M., Oleksyn, J., & Lee, T. D. (2009). Controls on declining carbon balance with leaf age among 10 woody species in Australian woodland: Do leaves have zero daily net carbon balances when they die? *New Phytologist*, 183, 153–166. <https://doi.org/10.1111/j.1469-8137.2009.02824.x>
- Reich, P. B., Tjoelker, M. G., Pregitzer, K. S., Wright, I. J., Oleksyn, J., & Machado, J. L. (2008). Scaling of respiration to nitrogen in leaves, stems and roots of higher land plants. *Ecology Letters*, 11, 793–801. <https://doi.org/10.1111/j.1461-0248.2008.01185.x>
- Reich, P. B., Uhl, C., Walters, M. B., & Ellsworth, D. S. (1991). Leaf lifespan as a determinant of leaf structure and function among 23 Amazonian tree species. *Oecologia*, 86, 16–24. <https://doi.org/10.1007/BF00317383>
- Restrepo-Coupe, N., Levine, N. M., Christoffersen, B. O., Albert, L. P., Wu, J., Costa, M. H., Galbraith, D., Imbuzeiro, H., Martins, G., da Araujo, A. C., Malhi, Y. S., Zeng, X., Moorcroft, P., & Saleska, S. R. (2017). Do dynamic global vegetation models capture the seasonality of carbon fluxes in the Amazon basin? A data-model intercomparison. *Global Change Biology*, 23, 191–208. <https://doi.org/10.1111/gcb.13442>
- Rocha, W., Metcalfe, D. B., Doughty, C. E., Brando, P., Silvério, D., Halladay, K., Nepstad, D. C., Balch, J. K., & Malhi, Y. (2014). Ecosystem productivity and carbon cycling in intact and annually burnt forest at the dry southern limit of the Amazon rainforest (Mato Grosso, Brazil). *Plant Ecology & Diversity*, 7, 25–40. <https://doi.org/10.1080/17550874.2013.798368>
- Rowland, L., Harper, A., Christoffersen, B. O., Galbraith, D. R., Imbuzeiro, H. M. A., Powell, T. L., Doughty, C., Levine, N. M., Malhi, Y., Saleska, S. R., Moorcroft, P. R., Meir, P., & Williams, M. (2015). Modelling climate change responses in tropical forests: Similar productivity estimates across five models, but different mechanisms and responses. *Geoscientific Model Development*, 8, 1097–1110. <https://doi.org/10.5194/gmd-8-1097-2015>
- Ryan, M. G. (1991). Effects of climate change on plant respiration. *Ecological Applications*, 1, 157–167. <https://doi.org/10.2307/1941808>
- Sakschewski, B., Von Bloh, W., Boit, A., Rammig, A., Kattge, J., Poorter, L., Peñuelas, J., & Thonicke, K. (2015). Leaf and stem economics



- spectra drive diversity of functional plant traits in a dynamic global vegetation model. *Global Change Biology*, 21, 2711–2725. <https://doi.org/10.1111/gcb.12870>
- Saxton, K. E., Rawls, W. J., Romberger, J. S., & Papendick, R. I. (1986). Estimating generalized soil-water characteristics from texture. *Soil Science Society of America Journal*, 50, 1031–1036. <https://doi.org/10.2136/sssaj1986.03615995005000040039x>
- Schleppi, P., Thimonier, A., & Walthert, L. (2011). Estimating leaf area index of mature temperate forests using regressions on site and vegetation data. *Forest Ecology and Management*, 261, 601–610. <https://doi.org/10.1016/j.foreco.2010.11.013>
- Sellers, P. J., Dickinson, R. E., Randall, D. A., Betts, A. K., Hall, F. G., Berry, J. A., Collatz, G. J., Denning, A. S., Mooney, H. A., & Nobre, C. A. (1997). Modeling the exchanges of energy, water, and carbon between continents and the atmosphere. *Science*, 275, 502–509. <https://doi.org/10.1126/science.275.5299.502>
- Smallman, T. L., Moncrieff, J. B., & Williams, M. (2013). WRFv3. 2-SPAv2: Development and validation of a coupled ecosystem-atmosphere model, scaling from surface fluxes of CO<sub>2</sub> and energy to atmospheric profiles. *Geoscientific Model Development*, 6, 1079–1093. <https://doi.org/10.5194/gmd-6-1559-2013>
- Smith, M. N., Stark, S. C., Taylor, T. C., Ferreira, M. L., Oliveira, E., Restrepo-Coupe, N., Chen, S., Woodcock, T., Santos, D. B., Alves, L. F., Figueira, M., Camargo, P. B., Oliveira, R. C., Aragão, L. E. O. C., Falk, D. A., McMahon, S. M., Huxman, T. E., & Saleska, S. R. (2019). Seasonal and drought-related changes in leaf area profiles depend on height and light environment in an Amazon forest. *New Phytologist*, 222, 1284–1297. <https://doi.org/10.1111/nph.15726>
- Stark, S. C., Leitold, V., Wu, J. L., Hunter, M. O., De Castilho, C. V., Costa, F. R. C., McMahon, S. M., Parker, G. G., Shimabukuro, M. T., Lefsky, M. A., Keller, M., Alves, L. F., Schiatti, J., Shimabukuro, Y. E., Brandão, D. O., Woodcock, T. K., Higuchi, N., de Camargo, P. B., de Oliveira, R. C., & Saleska, S. R. (2012). Amazon forest carbon dynamics predicted by profiles of canopy leaf area and light environment. *Ecology Letters*, 15, 1406–1414. <https://doi.org/10.1111/j.1461-0248.2012.01864.x>
- Street, L. E., Shaver, G. R., Williams, M., & Van Wijk, M. T. (2007). What is the relationship between changes in canopy leaf area and changes in photosynthetic CO<sub>2</sub> flux in arctic ecosystems? *Journal of Ecology*, 95, 139–150. <https://doi.org/10.1111/j.1365-2745.2006.01187.x>
- Sus, O., Williams, M., Bernhofer, C., Béziat, P., Buchmann, N., Ceschia, E., Doherty, R., Eugster, W., Grünwald, T., Kutsch, W., Smith, P., & Wattenbach, M. (2010). A linked carbon cycle and crop development model: Description and evaluation against measurements of carbon fluxes and carbon stocks at several European agricultural sites. *Agriculture, Ecosystems & Environment*, 139, 402–418. <https://doi.org/10.1016/j.agee.2010.06.012>
- Tang, H., & Dubayah, R. (2017). Light-driven growth in Amazon evergreen forests explained by seasonal variations of vertical canopy structure. *Proceedings of the National Academy of Sciences of the United States of America*, 114, 2640–2644. <https://doi.org/10.1073/pnas.1616943114>
- Thomas, R. Q., & Williams, M. (2014). A model using marginal efficiency of investment to analyze carbon and nitrogen interactions in terrestrial ecosystems. *Geoscientific Model Development*, 7, 2015–2037. <https://doi.org/10.5194/gmd-7-2015-2014>
- Thomas, R. Q., Williams, M., Cavaleri, M. A., Exbrayat, J. F., Smallman, T. L., & Street, L. E. (2019). Alternate trait-based leaf respiration schemes evaluated at ecosystem-scale through carbon optimization modeling and canopy property data. *Journal of Advances in Modeling Earth Systems*, 11(12), 4629–4644. <https://doi.org/10.1029/2019MSE001679>
- Thornton, P. E., & Zimmermann, N. E. (2007). An improved canopy integration scheme for a land surface model with prognostic canopy structure. *Journal of Climate*, 20, 3902–3923. <https://doi.org/10.1175/JCLI4222.1>
- Trugman, A. T., Anderegg, L. D. L., Sperry, J. S., Wang, Y., Venturas, M., & Anderegg, W. R. L. (2019). Leveraging plant hydraulics to yield predictive and dynamic plant leaf allocation in vegetation models with climate change. *Global Change Biology*, 12, 4008–4021. <https://doi.org/10.1111/gcb.14814>
- Trugman, A. T., Anderegg, L. D. L., Wolfe, B. T., Birami, B., Ruehr, N. K., Detto, M., Bartlett, M. K., & Anderegg, W. R. L. (2019). Climate and plant trait strategies determine tree carbon allocation to leaves and mediate future forest productivity. *Global Change Biology*, 10, 3395–3405. <https://doi.org/10.1111/gcb.14680>
- Van Loon, M. P., Schieving, F., Rietkerk, M., Dekker, S. C., Sterck, F., & Anten, N. P. R. (2014). How light competition between plants affects their response to climate change. *New Phytologist*, 203, 1253–1265. <https://doi.org/10.1111/nph.12865>
- Verheijen, L. M., Brövkén, V., Aerts, R., Bonisch, G., Cornelissen, J. H., Kattge, J., Reich, P. B., Wright, I. J., & Van Bodegom, P. M. (2013). Impacts of trait variation through observed trait-climate relationships on performance of an Earth system model: A conceptual analysis. *Biogeosciences*, 10, 5497–5515. <https://doi.org/10.5194/bg-10-5497-2013>
- Vico, G., Dralle, D., Feng, X., Thompson, S., & Manzoni, S. (2017). How competitive is drought deciduousness in tropical forests? A combined eco-hydrological and eco-evolutionary approach. *Environmental Research Letters*, 12, 065006. <https://doi.org/10.1088/1748-9326/aa6f1b>
- Violle, C., Navas, M. L., Vile, D., Kazakou, E., Fortunel, C., Hummel, I., & Garnier, E. (2007). Let the concept of trait be functional! *Oikos*, 116, 882–892. <https://doi.org/10.1111/j.0030-1299.2007.15559.x>
- Walker, A. P., Hanson, P. J., De Kauwe, M. G., Medlyn, B. E., Zaehle, S., Asao, S., Dietze, M., Hickler, T., Huntingford, C., & Iversen, C. M. (2014). Comprehensive ecosystem model-data synthesis using multiple data sets at two temperate forest free-air CO<sub>2</sub> enrichment experiments: Model performance at ambient CO<sub>2</sub> concentration. *Journal of Geophysical Research: Biogeosciences*, 119, 937–964. <https://doi.org/10.1002/2013JG002553>
- Waring, R. H., & Schlesinger, W. H. (1985). *Forest ecosystems. Concepts and management*. Academic Press.
- Weiss, M., Baret, F., Smith, G. J., Jonckheere, I., & Coppin, P. (2004). Review of methods for in situ leaf area index (LAI) determination: Part II. Estimation of LAI, errors and sampling. *Agricultural and Forest Meteorology*, 121, 37–53. <https://doi.org/10.1016/j.agrfor.2003.08.001>
- Williams, M., Bond, B. J., & Ryan, M. G. (2001). Evaluating different soil and plant hydraulic constraints on tree function using a model and sap flow data from ponderosa pine. *Plant, Cell & Environment*, 24, 679–690. <https://doi.org/10.1046/j.1365-3040.2001.00715.x>
- Williams, M., Malhi, Y., Nobre, A. D., Rastetter, E. B., Grace, J., & Pereira, M. G. P. (1998). Seasonal variation in net carbon exchange and evapotranspiration in a Brazilian rain forest: A modeling analysis. *Plant, Cell & Environment*, 21, 953–968. <https://doi.org/10.1046/j.1365-3040.1998.00339.x>
- Williams, M., Rastetter, E. B., Fernandes, D. N., Goulden, M. L., Wofsy, S. C., Shaver, G. R., Melillo, J. M., Munger, J. W., Fan, S. M., & Nadelhoffer, K. J. (1996). Modelling the soil-plant-atmosphere continuum in a *Quercus-Acer* stand at Harvard Forest: The regulation of stomatal conductance by light, nitrogen and soil/plant hydraulic properties. *Plant, Cell & Environment*, 19, 911–927. <https://doi.org/10.1111/j.1365-3040.1996.tb00456.x>
- Wright, I. J., Reich, P. B., Cornelissen, J. H. C., Falster, D. S., Groom, P. K., Hikosaka, K., Lee, W., Lusk, C. H., Niinemets, Ü., Oleksyn, J., Osada, N., Poorter, H., Warton, D. I., & Westoby, M. (2005). Modulation of leaf economic traits and trait relationships by climate. *Global Ecology and Biogeography*, 14, 411–421. <https://doi.org/10.1111/j.1466-822x.2005.00172.x>
- Wright, I. J., Reich, P. B., & Westoby, M. (2001). Strategy shifts in leaf physiology, structure and nutrient content between species of



- high-and low-rainfall and high- and low-nutrient habitats. *Functional Ecology*, 15, 423–434. <https://doi.org/10.1046/j.0269-8463.2001.00542.x>
- Wright, I. J., Reich, P. B., Westoby, M., Ackerly, D. D., Baruch, Z., Bongers, F., Cavender-Bares, J., Chapin, T., Cornelissen, J. H., Diemer, M., Flexas, J., Garnier, E., Groom, P. K., Gulias, J., Hikosaka, K., Lamont, B. B., Lee, T., Lee, W., Lusk, C., ... Villar, R. (2004). The worldwide leaf economics spectrum. *Nature*, 428, 821–827. <https://doi.org/10.1038/nature02403>
- Wright, I. J., & Westoby, M. (2002). Leaves at low versus high rainfall: Coordination of structure, lifespan and physiology. *New Phytologist*, 155, 403–416. <https://doi.org/10.1046/j.1469-8137.2002.00479.x>
- Wright, J. K., Williams, M., Starr, G., Mcgee, J., & Mitchell, R. J. (2013). Measured and modelled leaf and stand-scale productivity across a soil moisture gradient and a severe drought. *Plant Cell and Environment*, 36, 467–483. <https://doi.org/10.1111/j.1365-3040.2012.02590.x>
- Wu, J., Albert, L. P., Lopes, A. P., Restrepo-Coupe, N., Hayek, M., Wiedemann, K. T., Guan, K., Stark, S. C., Christoffersen, B., Prohaska, N., Tavares, J. V., Marostica, S., Kobayashi, H., Ferreira, M. L., Campos, K. S., Da Silva, R., Brando, P. M., Dye, D. G., Huxman, T. E., ... Saleska, S. R. (2016). Leaf development and demography explain photosynthetic seasonality in Amazon evergreen forests. *Science*, 351, 972–976. <https://doi.org/10.1126/science.aad5068>
- Xu, B., Park, T., Yan, K., Chen, C., Zeng, Y., Song, W., Yin, G., Li, J., Liu, Q., Knyazikhin, Y., & Myneni, R. (2018). Analysis of global LAI/FPAR products from VIIRS and MODIS sensors for spatio-temporal consistency and uncertainty from 2012–2016. *Forests*, 9, 73. <https://doi.org/10.3390/f9020073>
- Xu, L., & Baldocchi, D. D. (2004). Seasonal variation in carbon dioxide exchange over a Mediterranean annual grassland in California. *Agricultural and Forest Meteorology*, 123, 79–96. <https://doi.org/10.1016/j.agrformet.2003.10.004>
- Xu, X., Medvigy, D., Joseph Wright, S., Kitajima, K., Wu, J., Albert, L. P., Martins, G. A., Saleska, S. R., & Pacala, S. W. (2017). Variations of leaf longevity in tropical moist forests predicted by a trait-driven carbon optimality model. *Ecology Letters*, 20, 1097–1106. <https://doi.org/10.1111/ele.12804>
- Xu, X., Medvigy, D., Powers, J. S., Becknell, J. M., & Guan, K. (2016). Diversity in plant hydraulic traits explains seasonal and inter-annual variations of vegetation dynamics in seasonally dry tropical forests. *New Phytologist*, 212, 80–95. <https://doi.org/10.1111/nph.14009>

## SUPPORTING INFORMATION

Additional supporting information may be found online in the Supporting Information section.

**How to cite this article:** Flack-Prain S, Meir P, Malhi Y, Smallman TL, Williams M. Does economic optimisation explain LAI and leaf trait distributions across an Amazon soil moisture gradient? *Glob Change Biol*. 2021;27:587–605. <https://doi.org/10.1111/gcb.15368>